BALLISTIC RESEARCH LABORATORIES

MEMORANDUM REPORT NO. 1916

MARCH 1968

AIR SHOCK FILLING OF MODEL ROOMS

George A. Coulter

Terminal Ballistics Laboratory

RDT&E Project No. 1T014501A33E

ABERDEEN PROVING GROUND, MARYLAND

BRL MR 1916

BRL

AD

MEMORANDUM REPORT NO. 1916

AIR SHOCK FILLING OF MODEL ROOMS

by

George A. Coulter

March 1968

U. S. ARMY MATERIEL COMMAND
BALLISTIC RESEARCH LABORATORIES
ABERDEEN PROVING GROUND, MARYLAND

FOREWORD

The work reported here was begun in support of the assigned mission of the Terminal Ballistics Laboratory (TBL). The work was slanted toward a study for the Office of Civil Defense (OCD Work Unit 1123 C) which was being conducted at the same time and which could derive direct benefit.

BALLISTIC RESEARCH LABORATORIES

MEMORANDUM REPORT NO. 1916

GACoulter/sjw
Aberdeen Proving Ground, Md.
March 1968

AIR SHOCK FILLING OF MODEL ROOMS

ABSTRACT

The results of model room and chamber filling are given for two- and three-dimensional models exposed to shock waves 5-20 psi overpressure produced in the 4 x 15 in. and 24 in. shock tubes. Additional results are given for a field experiment in which a 3 ft cubic room was exposed to a 5 psi overpressure blast wave from the explosion of 100 tons of TNT. The results are presented on pressure-time filling records and on high speed photographs. A smoke grid technique was used to illustrate the shock filling process.

TABLE OF CONTENTS

LIST OF FIGURES AND TABLES

LIST OF FIGURES AND TABLES (Continued)

LIST OF FIGURES AND TABLES (Continued)

LIST OF FIGURES AND TABLES (Continued)

LIST OF SYMBOLS

A	Area of entrance to model
P_{fill}	Pressure to which chamber fills
P_S	Side-on overpressure of input shock wave
P'_S	Side-on overpressure of diffracted shock wave
T	Time
V	Volume of model

I. INTRODUCTION

The experiments reported in this memorandum report were designed to determine the important parameters of the blast wave filling process of rooms. To further the understanding of the filling process, two- and three-dimensional model rooms were constructed and tested in the shock tubes at the Ballistic Research Laboratories (BRL) Shock Tube Facility, through a shock overpressure range of 5 to 20 psi. As a check of the model scaling, a 3 ft cube model was exposed to filling from the blast wave produced by the explosion of a 100 ton of TNT during Shot 6 of the Canadian Distant Plain Series in July 1967.

Filling of the two-dimensional models was recorded by high speed framing cameras and by piezoelectric pressure transducers. In all the three-dimensional models, pressure transducers only recorded the filling as a function of time. The results of the high speed photography are shown in Appendix A and the pressure time records in Appendices B and C. Appendix D contains the results of the machine calculations for the motion of the smoke grids in the disturbed flow field within the two-dimensional models. Tables and flow vectors are given in this appendix.

Comparison of plots of the filling data are given in the Result Section illustrating the filling of the model as a function of orientation to the shock wave, type and number of entrances, and size and number of rooms.

The analysis of the experimental data and computer predictions for several typical models will be published separately as Reference 1.*

II. EXPERIMENTS

Three types of models were used for the present experiments: (a) three-dimensional models exposed to shock waves produced in the 24 in. shock tube, (b) two-dimensional models placed in the optical

References are listed on page 63.

test section of the 4 x 15 in. shock tube, and (c) a field model exposed to the blast wave produced by a large explosion of TNT. Table I summarizes the models and the conditions of the test.

A. Three-Dimensional Models

A series of three-dimensional models were designed and tested in the 24 in. shock tube to determine the comparative importance of filling parameters such as orientation to the shock wave, type and number of entrances, size and number of rooms, and strength of shock wave applied to the model.

Models I-IV were filled by the shock wave while attached to the outside of the test section. Both side-on and stagnation filling were used with entrance diameters of 1/2 in. and 2 in., interior volume to entrance area ratio of 435 ft and 27.2 ft. The remaining three-dimensional models, V-XIII, were placed inside the shock tube test section. Figures 1-6 show representative models given in Table I. Figure 7 shows typical undisturbed pressure-time records from the 24 in. shock tube test section without a model in the test section. Examples are shown for side-on overpressure (upper trace) and stagnation overpressure as measured by a pitot tube gage (bottom trace) at the 5, 10 and 20 psi test range. These are representative of the input pressures applied to the models.

B. Two-Dimensional Models

In order to observe the dependence of shock waves expansion and associated flow into a model as a function of entrance width, the two-dimensional model shown in Figure 8 was built. Figure 8-A shows the basic full reflection model, 8-B, a variable smoke grid which acted as a flow indicator, and 8-C shows the pressure transducer array used to monitor pressure as a function of time.

A complete description of the smoke grid technique may be found in Reference 2. Briefly, cigarette smoke is pulled through the model in vertical and crossing horizontal directions (streams do not touch) by means of a vacuum pump. The streams and shock wave are photographed with a Dynafax Model 326-3 high speed framing camera after the shock wave has

Table I. Experimental Models

Model No.	Size	Type of Filling	Input Pressure (psi)	V/A (ft)	Type of Entrance
		Three-dimensional models outside shock tube			
I	8 1/8 in. dia x 19 3/4 in.	Side	10, 20	435	1/2 in. dia
II	Same	Side	10, 20	27.2	2 in. dia
III	Same	2 x 4 x 4 in. Stagnation Block	10, 20	435	1/2 in. dia
IV	Same	3 1/2 x 3 1/2 x 3 1/6 in. Stagnation Block	10, 20	27.2	2 in. dia
		Three-dimensional models inside shock tube			
V	4 in. cube	Front, Side, or Rear	10, 20	1.65	1.2 x 2.7 in.
VI	Same	Front, Side, or Rear	10, 20	27.4	0.3 x 0.65 in.
VII	Two 4 in. cubic rooms	Front, Side, or Rear	10, 20	27.4 ea	0.3 x 0.65 in.
VIII	4 1/2 in. cube (outside)	None (loading only)	5, 10, 20	----	----------
IX	4 in. cube	Front	5, 10, 20	54.8	Two 0.15 x 0.325 in. spaced 1.333 in.
X	4 1/2 in. cube (outside)	w/4 1/2 x 4 1/2 x 8 3/4 in. shield	5, 10, 20	----	----------
XI	4 in. cube	Front	5, 10, 20	27.4	Two 0.3 x 0.325 in. spaced 1.333 in.
XII	4 1/2 in. cube (outside)	Front	5, 10, 20	NA	None 0.3 x 0.65 in. 1.2 x 2.7 in.
XIII	4 in. cube	Front and Rear	5, 10, 20	27.4	Two 0.3 x 0.325 in.

Table I. Experimental Models (Continued)

Model No.	Size	Type of Filling	Input Pressure (psi)	V/A (ft)	Type of Entrance
		Two-dimensional models inside shock tube			
XIV-A		Front (reflection plate)	5	10.7	1/8 x 4 in.
XIV-B			5	5.33	1/4 x 4 in.
XIV-C			5	2.67	1/2 x 4 in.
XIV-D			5	1.33	1 x 4 in.
XIV-E			5	0.67	2 x 4 in.
XIV-F			5	0.67	Two 1 x 4 in. spaced 0.667 in.
		Field model			
XV	36 in. cube	Front	5	27.4	0.702 x 1.403 ft

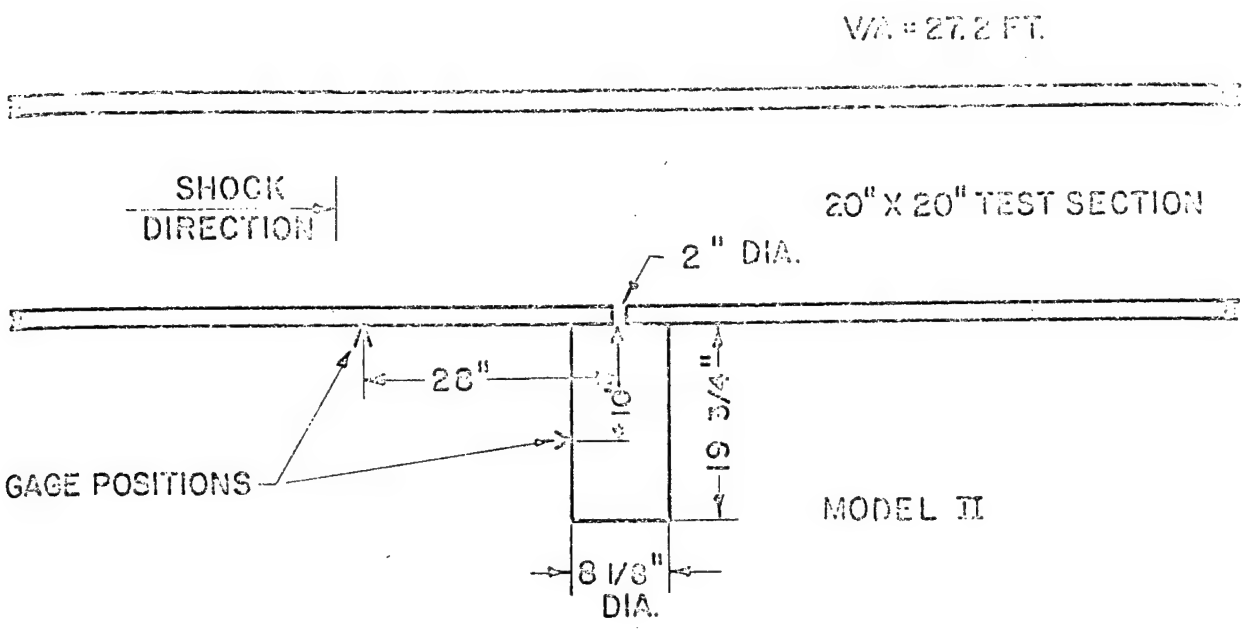

(A) SIDE-ON ENTRANCE MODEL OUTSIDE OF TEST SECTION

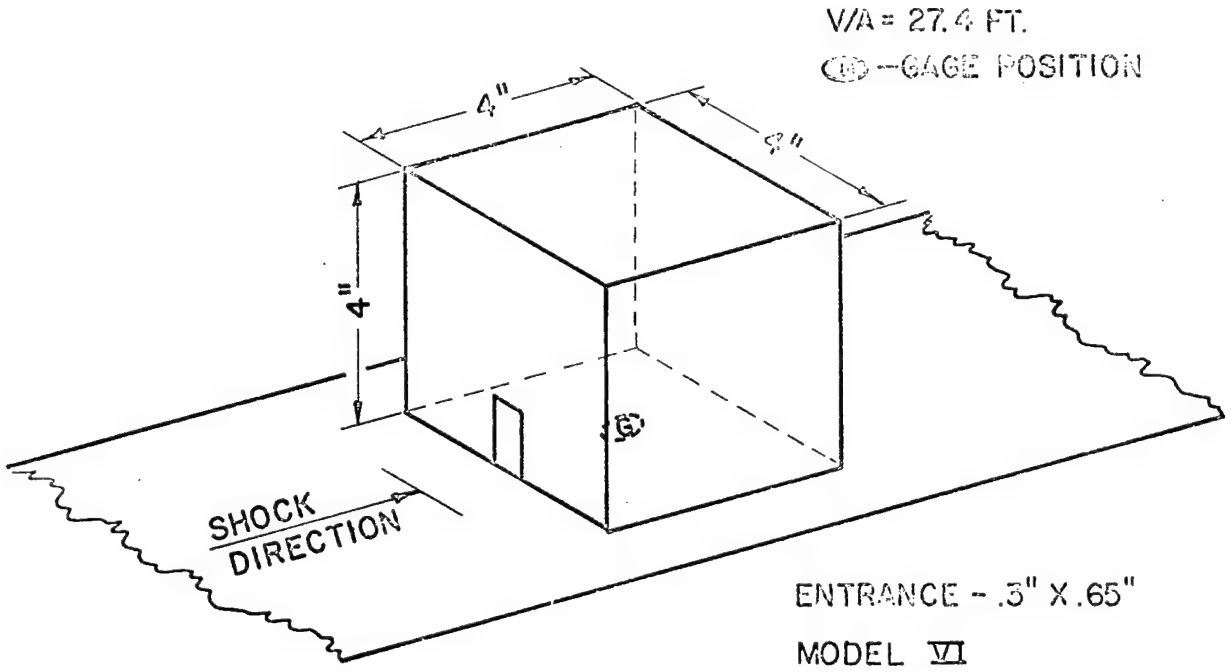

(B) FRONT ENTRANCE

Figure 1. Positions of models for comparing entrance orientations

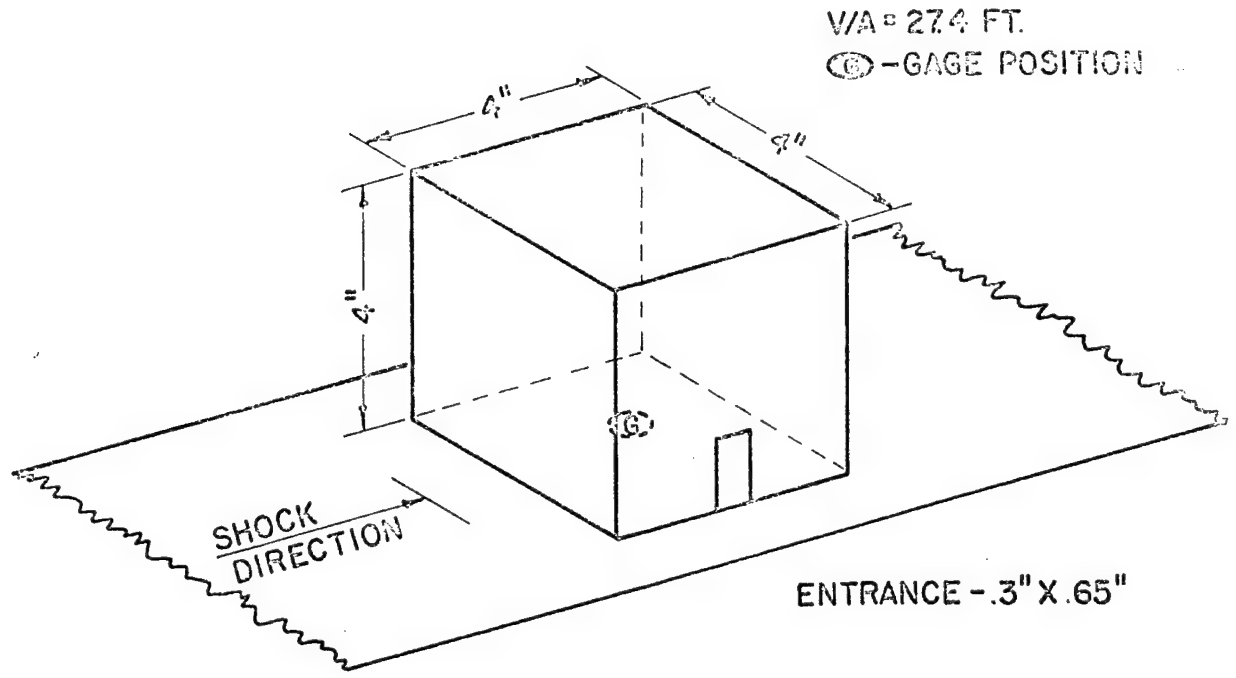

(C) SIDE ENTRANCE

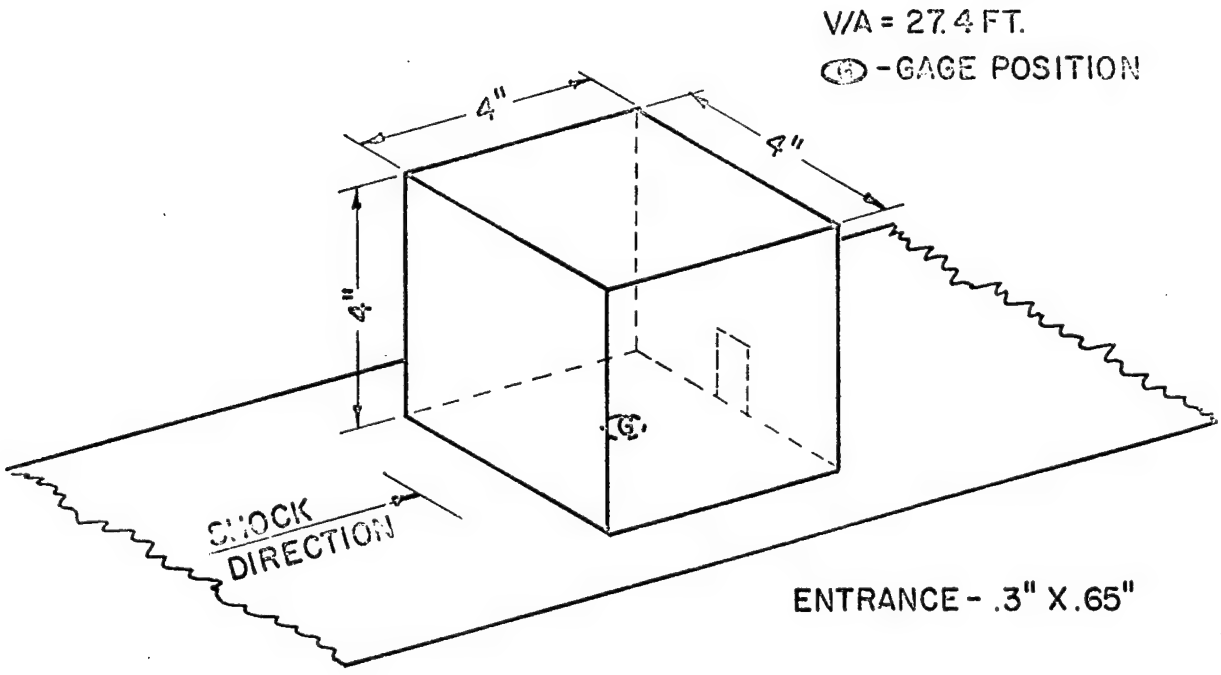

(D) REAR ENTRANCE

Figure 1. Positions of models for comparing entrance orientations (Continued)

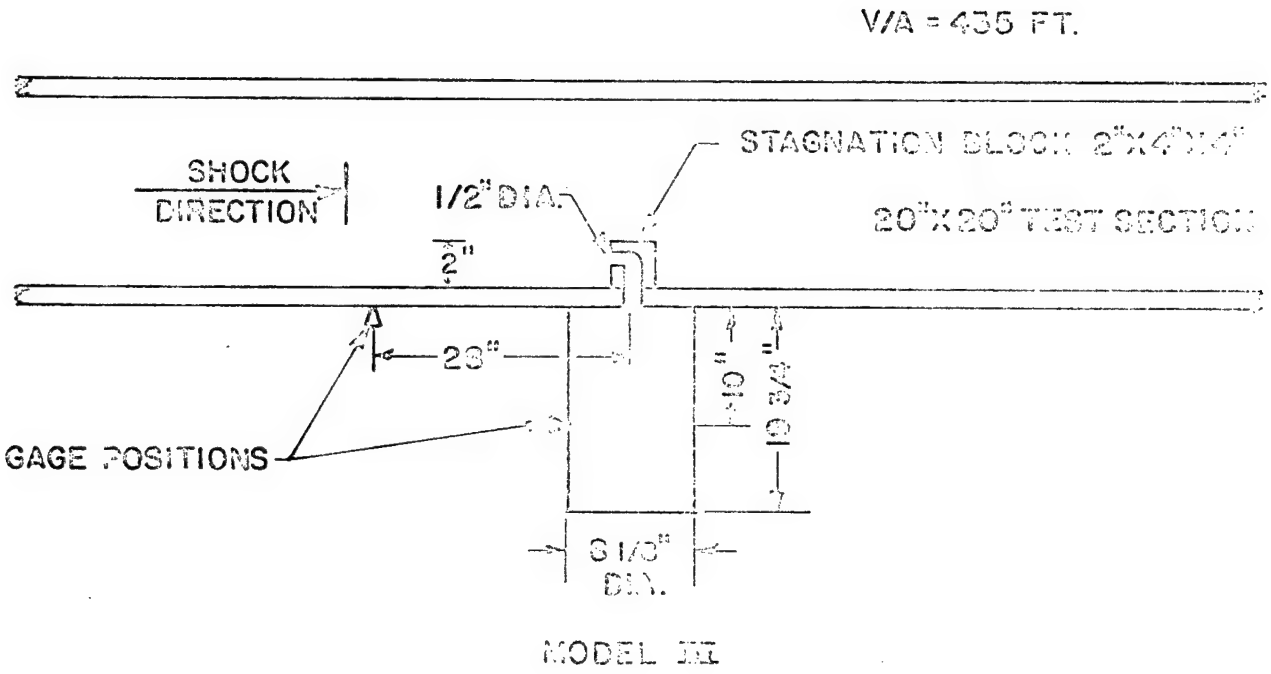

Figure 2. Stagnation entrance model outside of test section

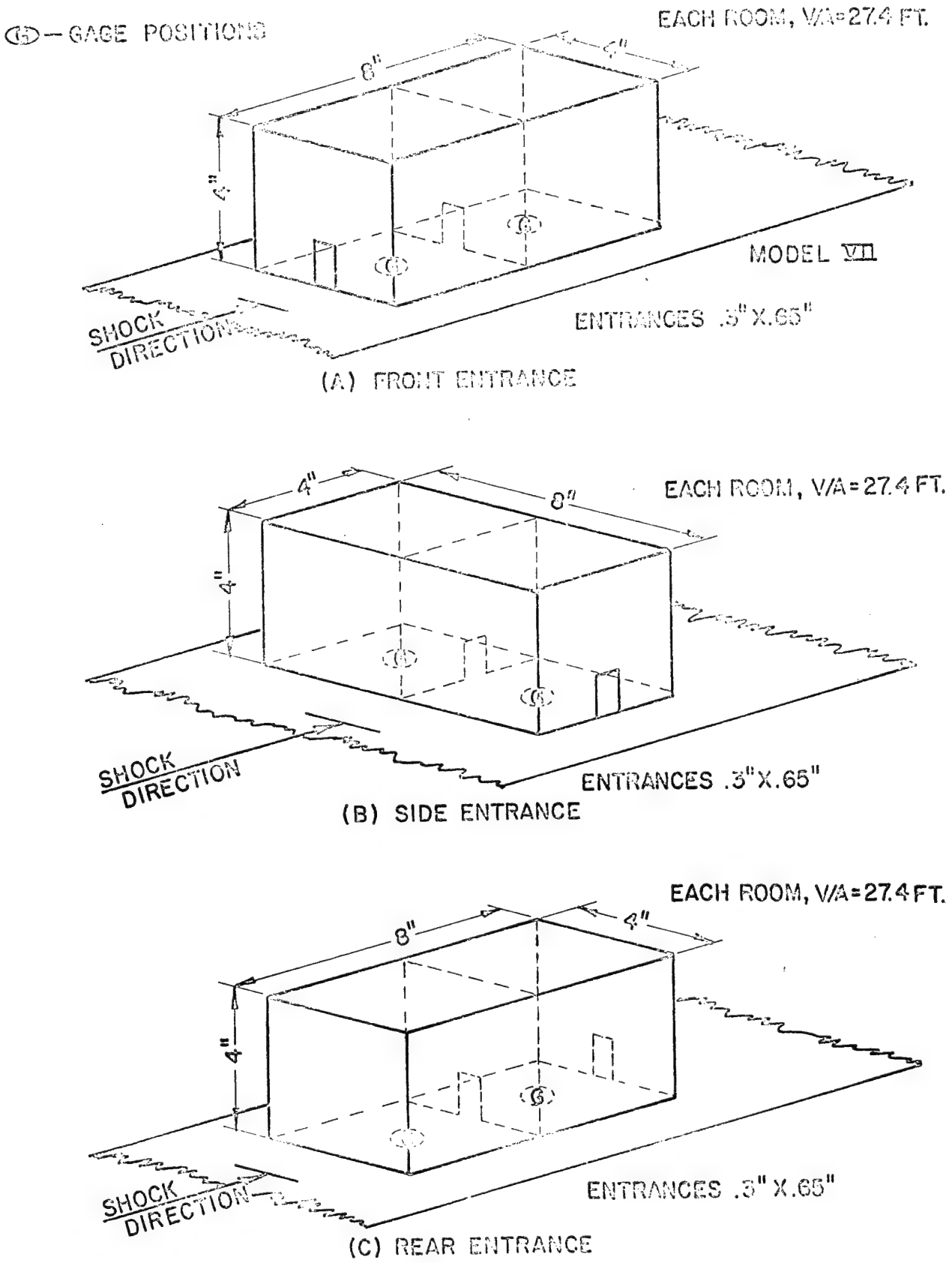

Figure 3. Two-room model used in fill-time test

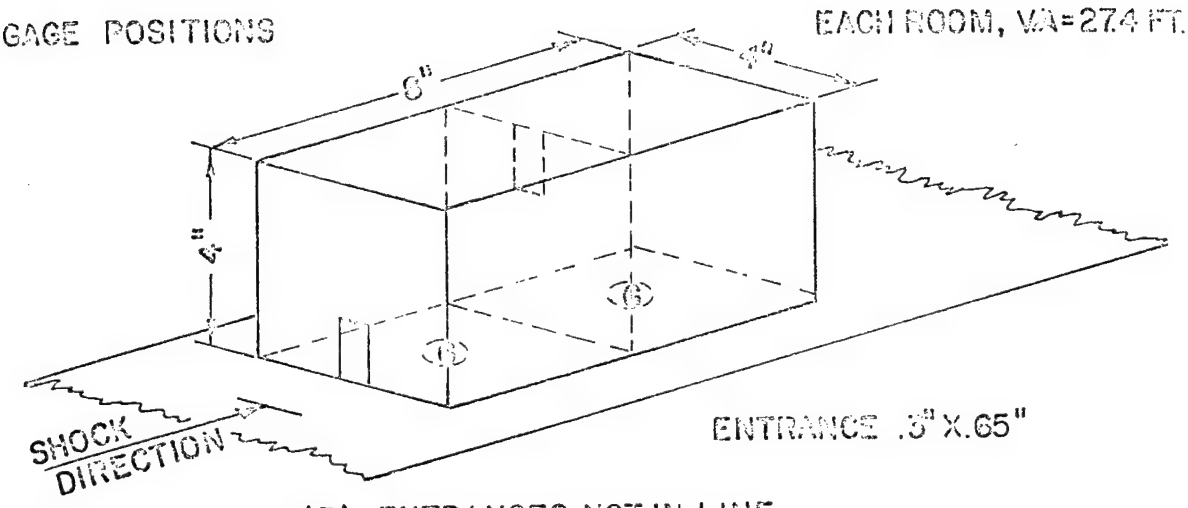

(D) ENTRANCES NOT IN LINE

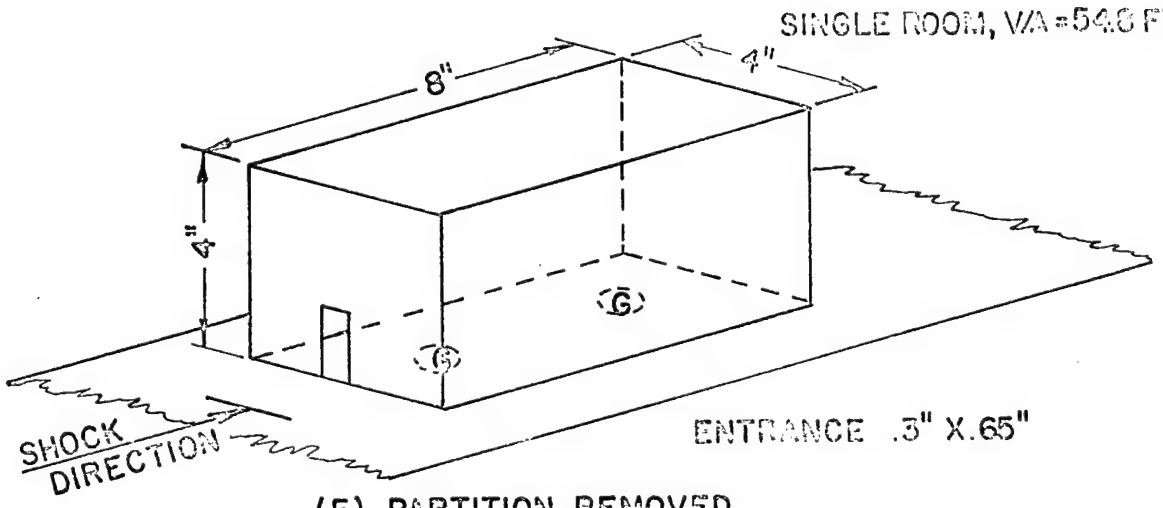

(E) PARTITION REMOVED

Figure 3. Two-room model used in fill-time test (Continued)

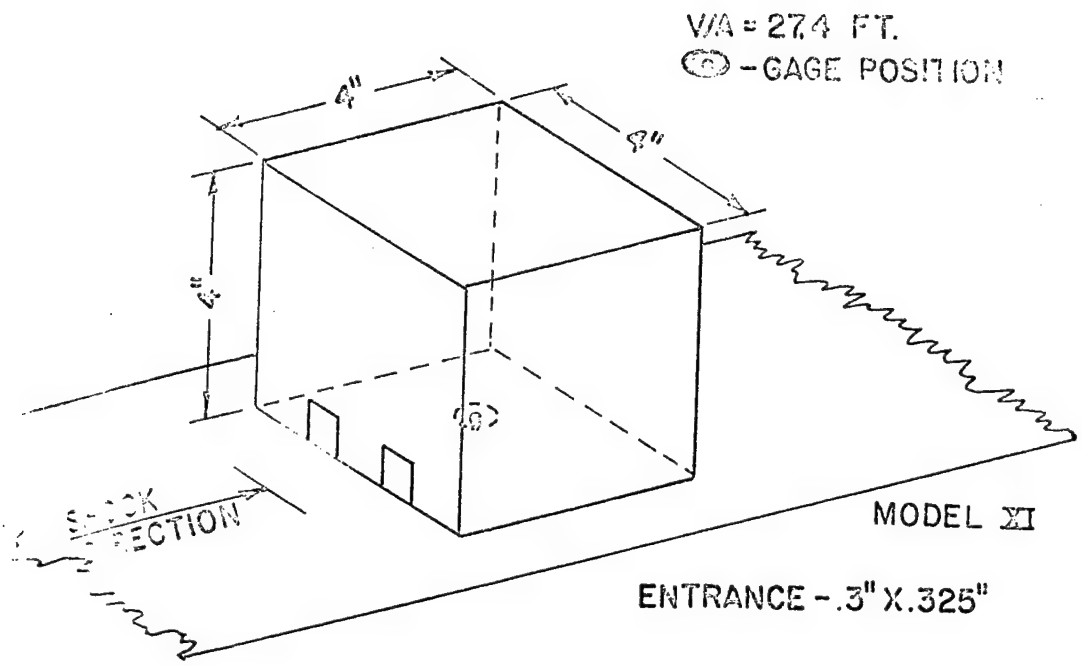

(A) DOUBLE ENTRANCE

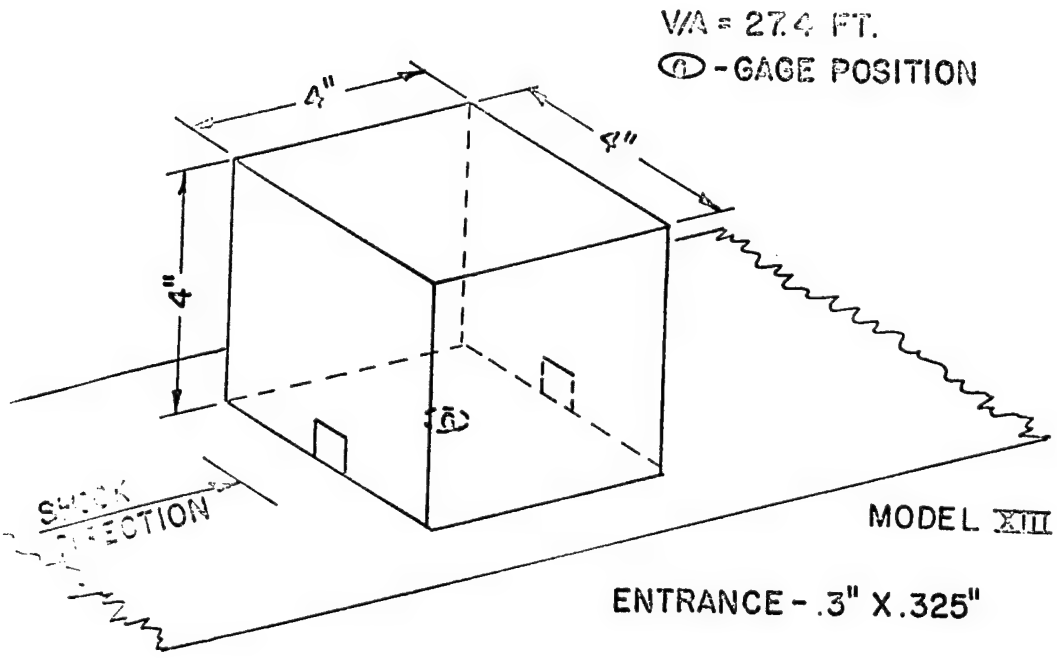

(B) FRONT AND REAR ENTRANCE

Figure 4. Models with two entrances

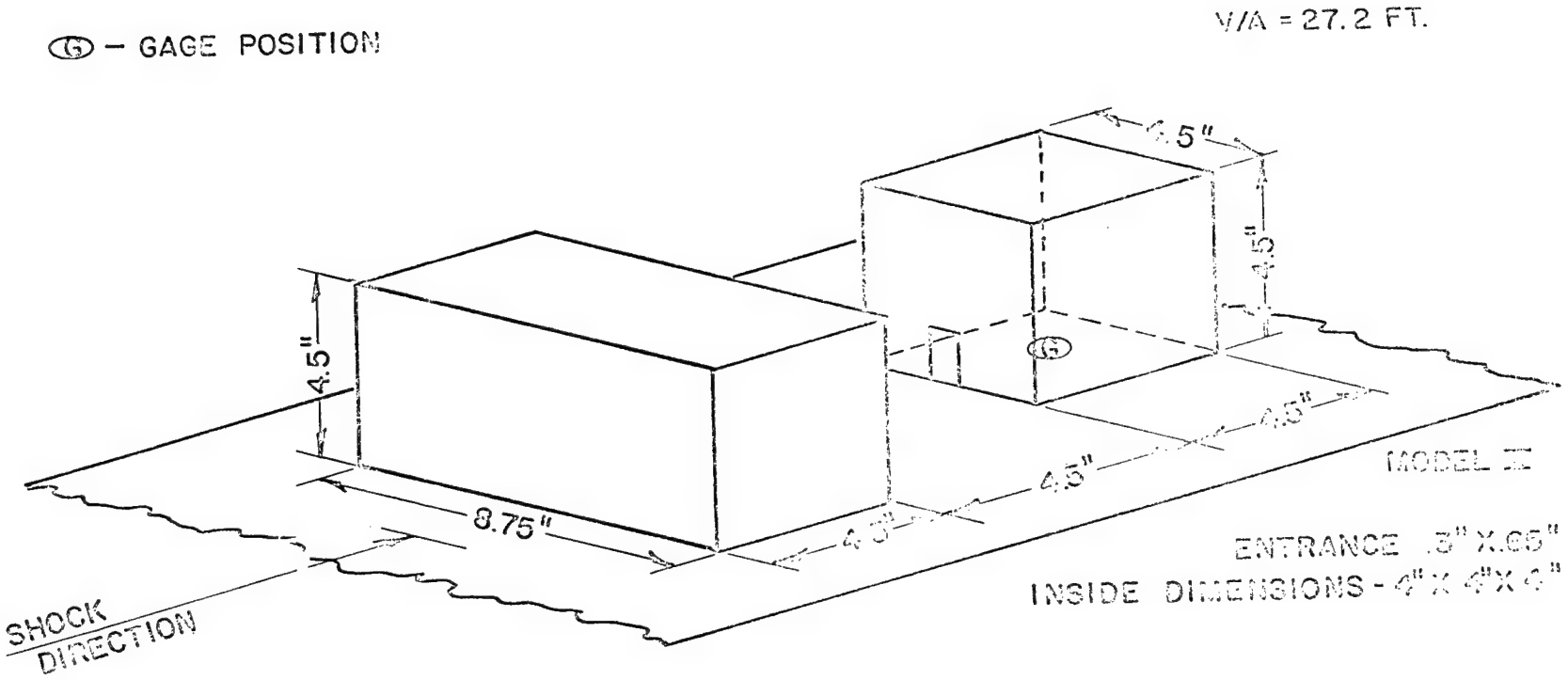

Figure 5. Model placed behind a shield a distance equal to one shield-height

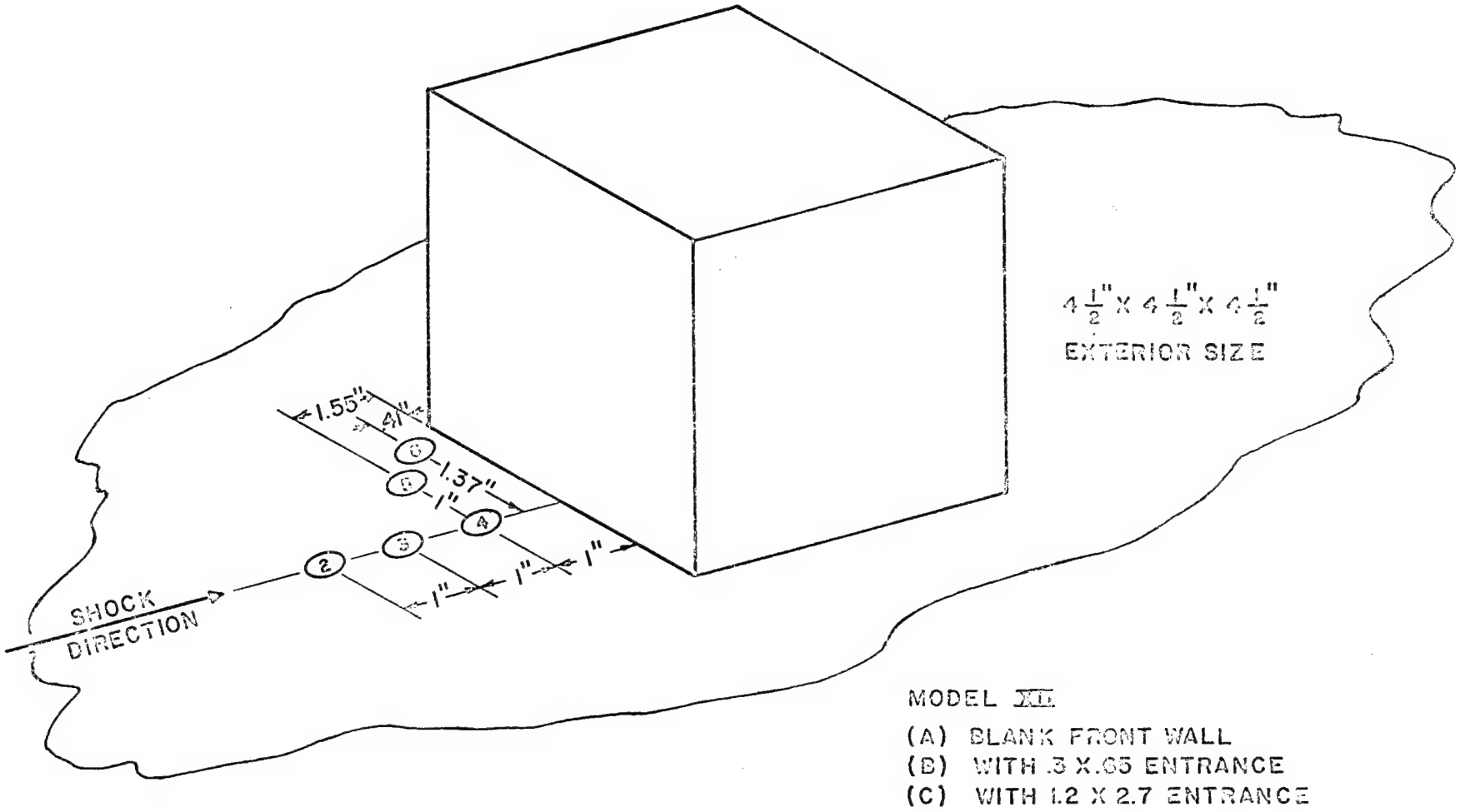

Figure 6. Model XII-upstream ground loading

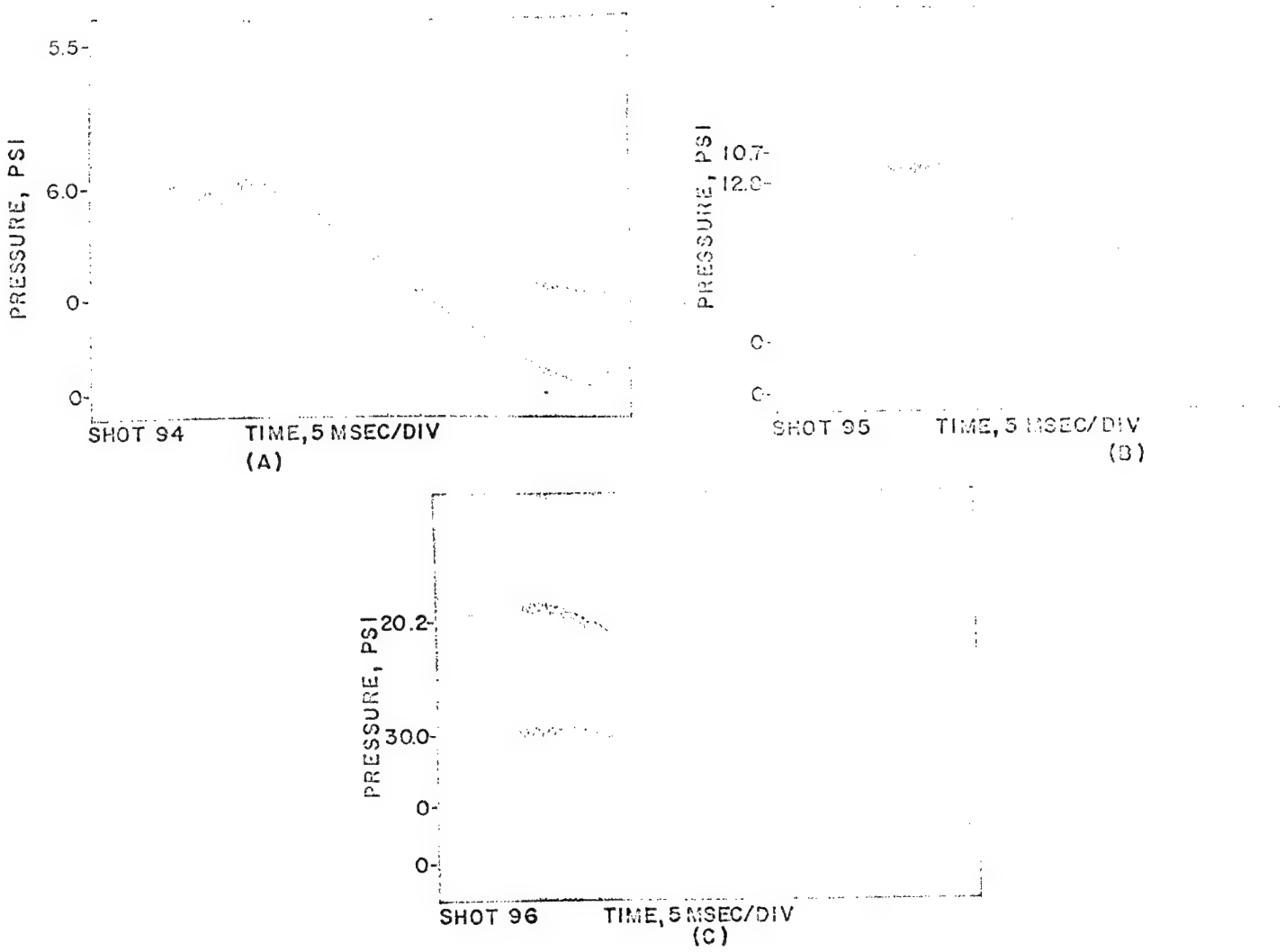

Figure 7. Shock side-on and stagnation overpressure input records

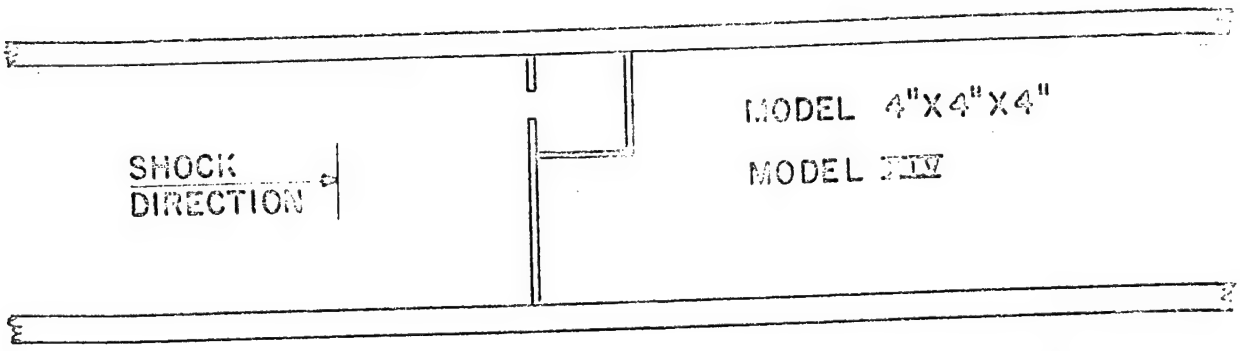

(A) BASIC MODEL FOR TWO-DIMENSIONAL EXPERIMENTS

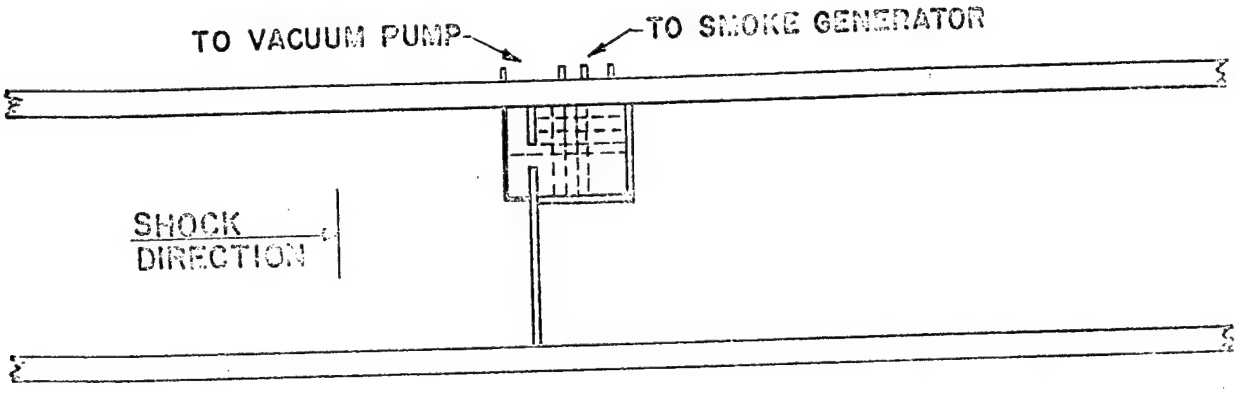

(B) SMOKE GRID GENERATOR

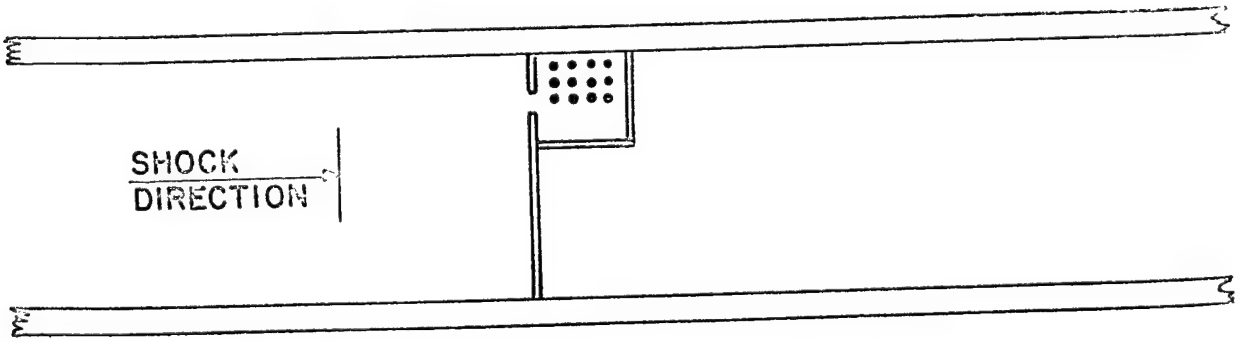

(C) PRESSURE TRANSDUCER POSITIONS

Figure 8. Two-dimensional model used with the smoke streams

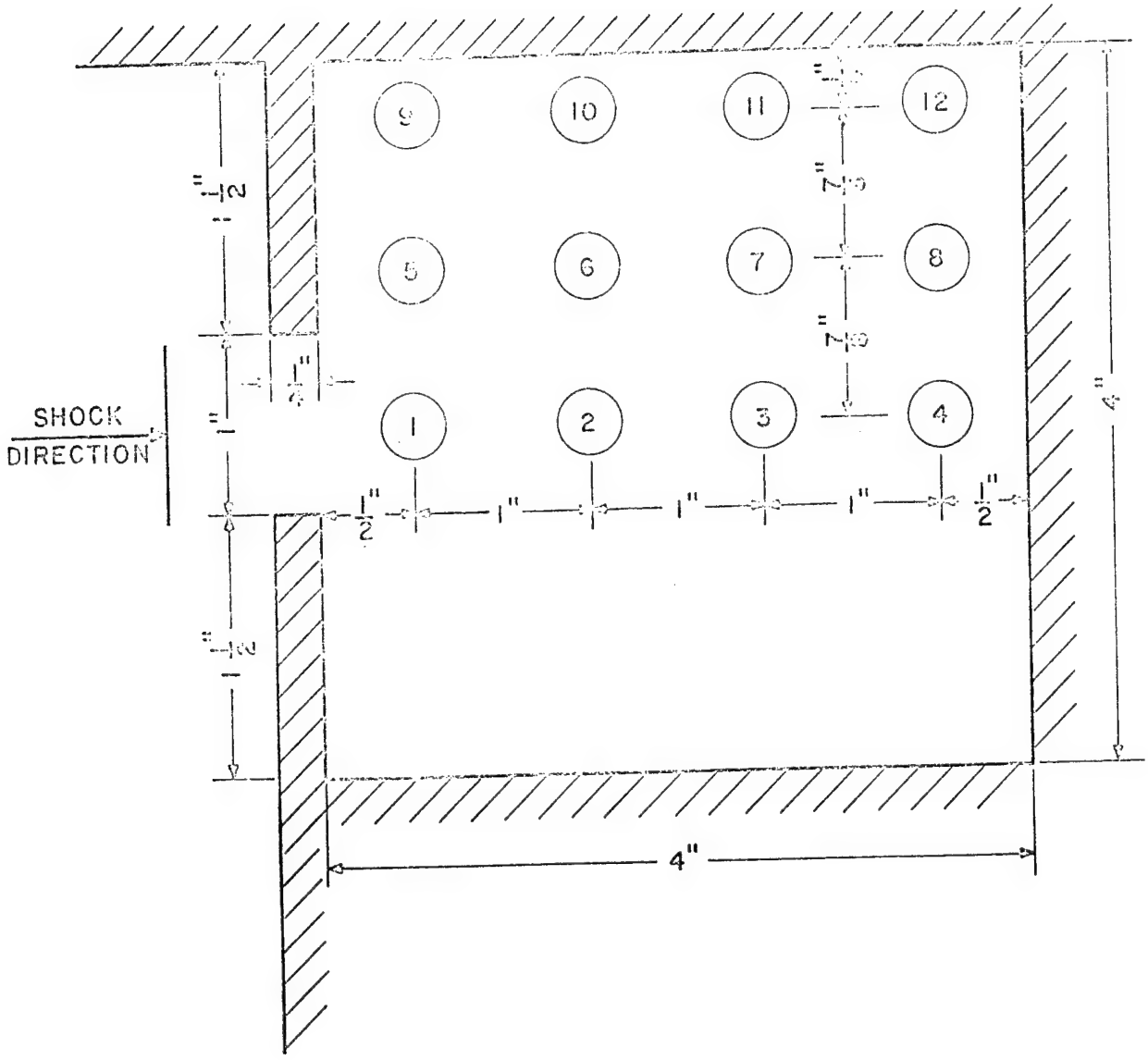

(D) 4"X 15" SHOCK TUBE GAGE POSITIONS-MODEL IV-D

Figure 8. Two-dimensional model used with the smoke streams (Continued)

entered the model. Average flow speed, direction, and density may be calculated from the smoke displacement and the known camera frame time separation and conditions of ambient density.

The pressure transducer instrumentation used for the experiment has been described in Reference 3. It consisted of ceramic pressure transducers, charge amplifiers, and Tektronic oscilloscopes with Polaroid cameras which recorded the pressure-time traces. Figure 8-D shows the transducer spacing and numbering system that was used for Model XIV. This numbering is followed in Table A-I of Appendix A and in Appendix C.

A single shot (No. 151 of Table A-III, Appendix A) illustrates the path given to a nylon ball caught in the flow after the shock wave has passed the ball. An entrance of 1 in. width was used for this shot. The results are given as distance time plots in the Result Section.

C. Field Model

Figure 9 shows a sketch of the field model which was exposed to the blast from 100 tons of TNT during Shot 6 of the Canadian Distant Plain series in July 1967. The model was made of 2 in. thick plywood reinforced with angle iron. The entrance was 0.7 x 1.4 ft corresponding to the volume to area ratio of the 4 in. cube of Model VI. (See Table I.)

A peak overpressure of approximately 5 psi was expected for the blast wave at the models position on the blast line. Gage positions are shown in Figure 9 where pressure records were obtained. An additional position, not shown, was taken from the blast line transducers to show an undisturbed input wave. The general instrumentation used for the entire Distant Plain series, including this model, may be found in Reference 4.

The pressure-time traces for Model XV are presented in the Result Section of this report.

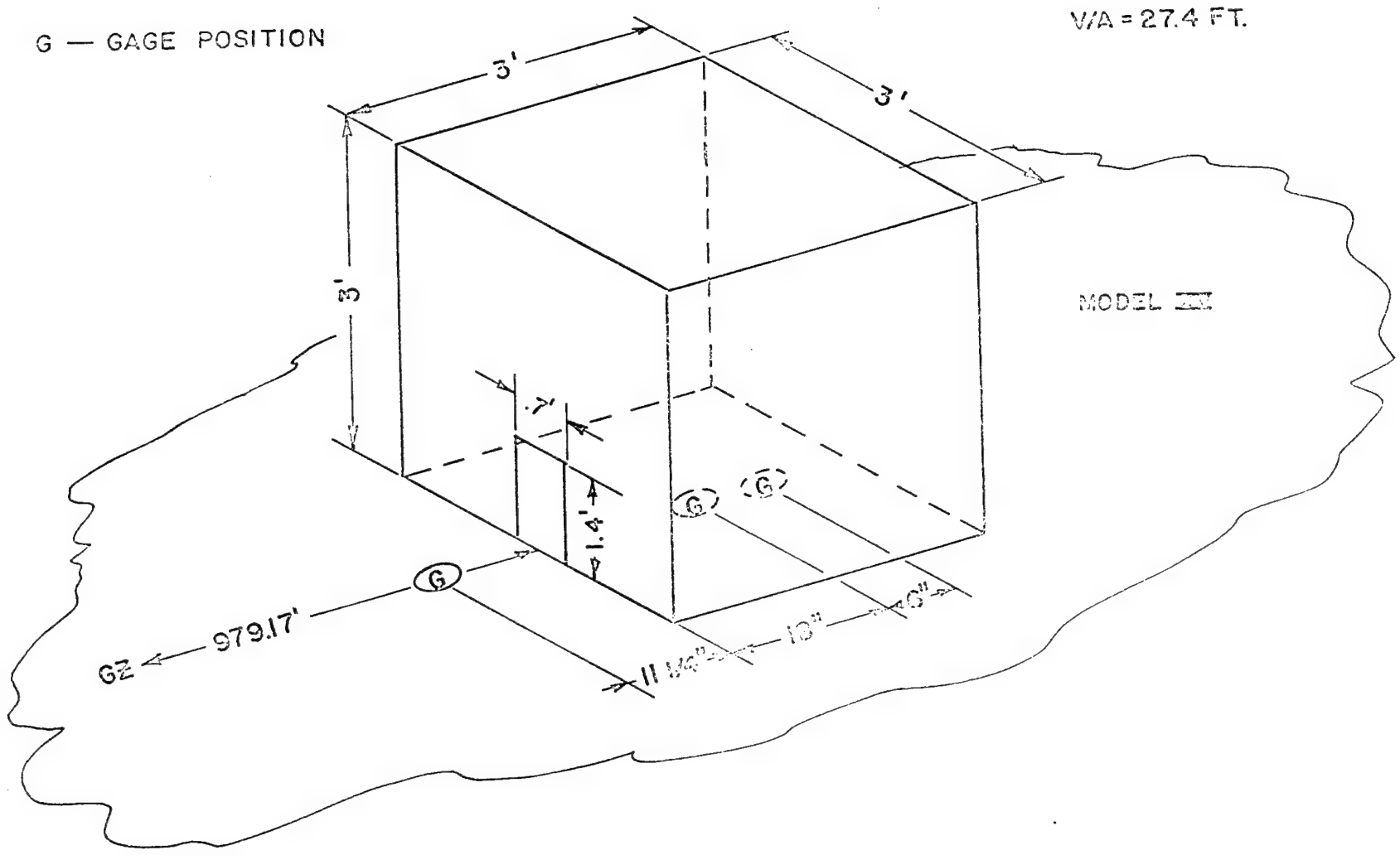

Figure 9. Field model exposed to blast from 100 tons of TNT

III. RESULTS

The results of the experiment are discussed in an order corresponding to the previous experimental parts.

A. Three-Dimensional Models

The tabulated results for the three-dimensional models are shown by model number in Table B-I, Appendix B. The various models and shots have been grouped for plotting according to the parameter the filling process is dependent upon.

Figures 10 and 11 show comparison plots of filling as a function of model orientation to the shock wave, and as a function of type of filling for Models II, IV, and VI. Nominal 10 and 20 psi side-on input waves are shown as applied to the models with volume to area (V/A) ratio of 27.2 ft. One can see a closer grouping of fill curves for P_s = 10 psi than for 20 psi, but the stagnation block filling outside of the test section corresponds roughly to the front fill inside the test section. Again the side-on filling for the model outside of the test section is similar to the rear-on filling for the model inside the shock tube. The side-on filling for the model in the shock tube is the lowest value of all orientations, or types of filling.

Figure 12 compares the filling curves for different values of V/A. Models III, V, VI, and VII are compared for ratios of V/A = 1.65 ft to 435 ft. The maximum pressure to which the models filled varied from 14 psi at 1.5 msec for the smallest V/A to about 1.3 psi at 56 msec for the largest V/A tested.

Figure 13 shows the filling of Model VI as a function of input side-on overpressure. Notice that the fill time to maximum pressure becomes greater as the input pressure increases, from 13.7 msec to 17.2 msec. Also, the maximum fill pressure is not quite the value of the input record; but the fill pressure would become greater if the input flat duration were longer. Notice, however, the overshoot of the filling pressure with respect to the side-on input record, but it is less than the stagnation overpressure corresponding to the input pressures. See

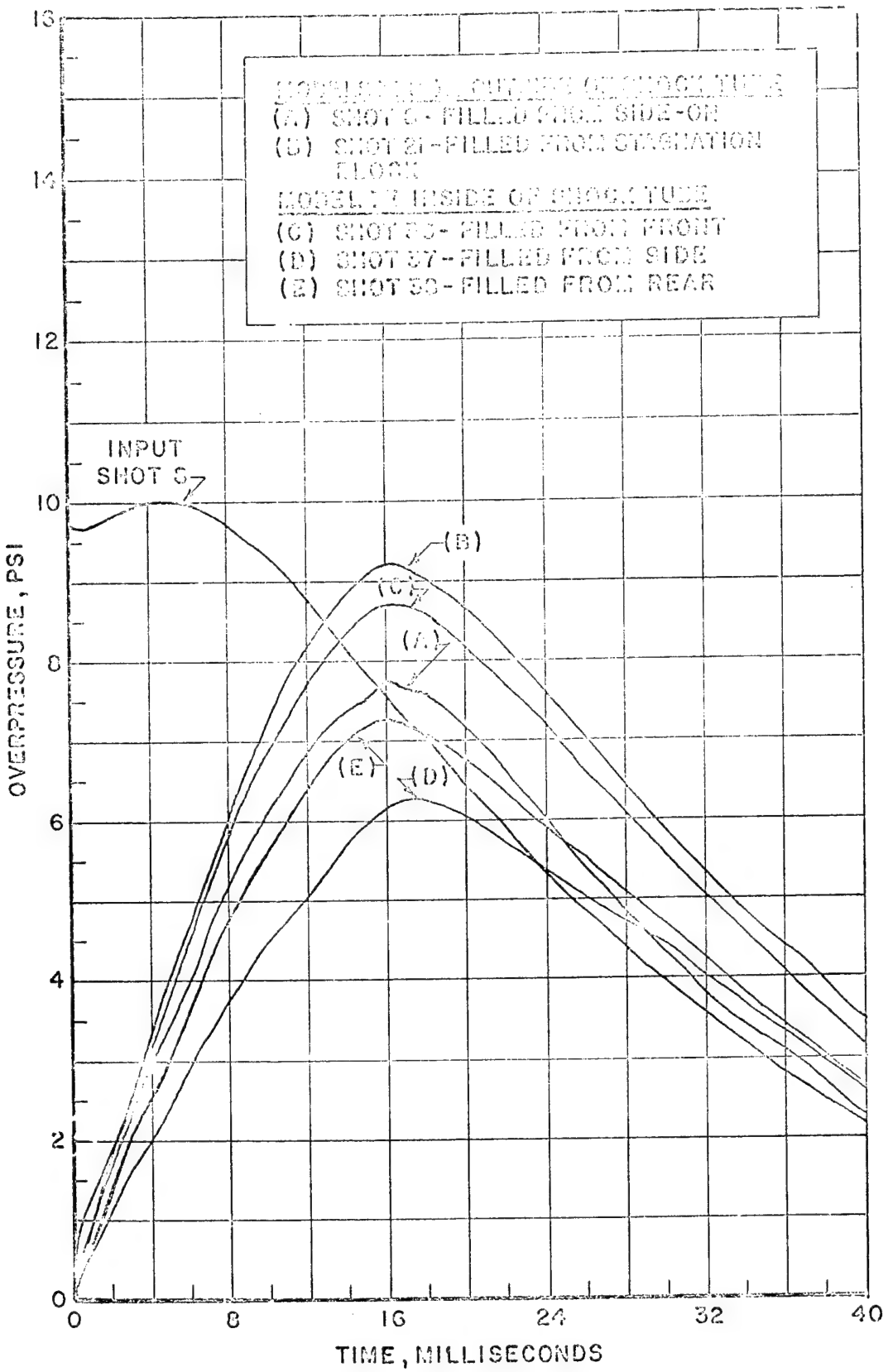

Figure 10. Comparison of filling as a function of orientation to shock wave, P_s = 9.8 psi

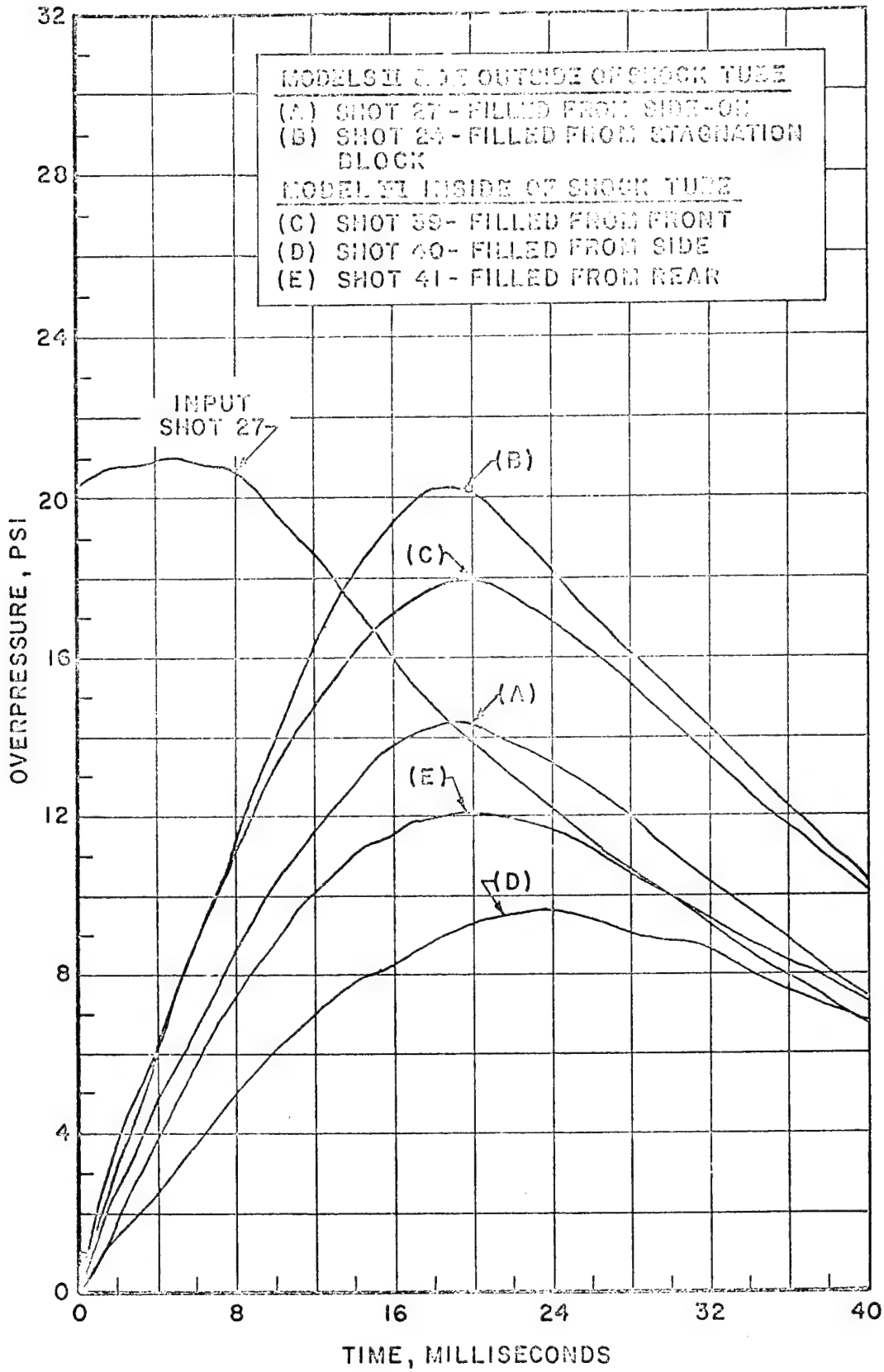

Figure 11. Comparison of filling as a function of orientation to shock wave, P_s = 20.5 psi

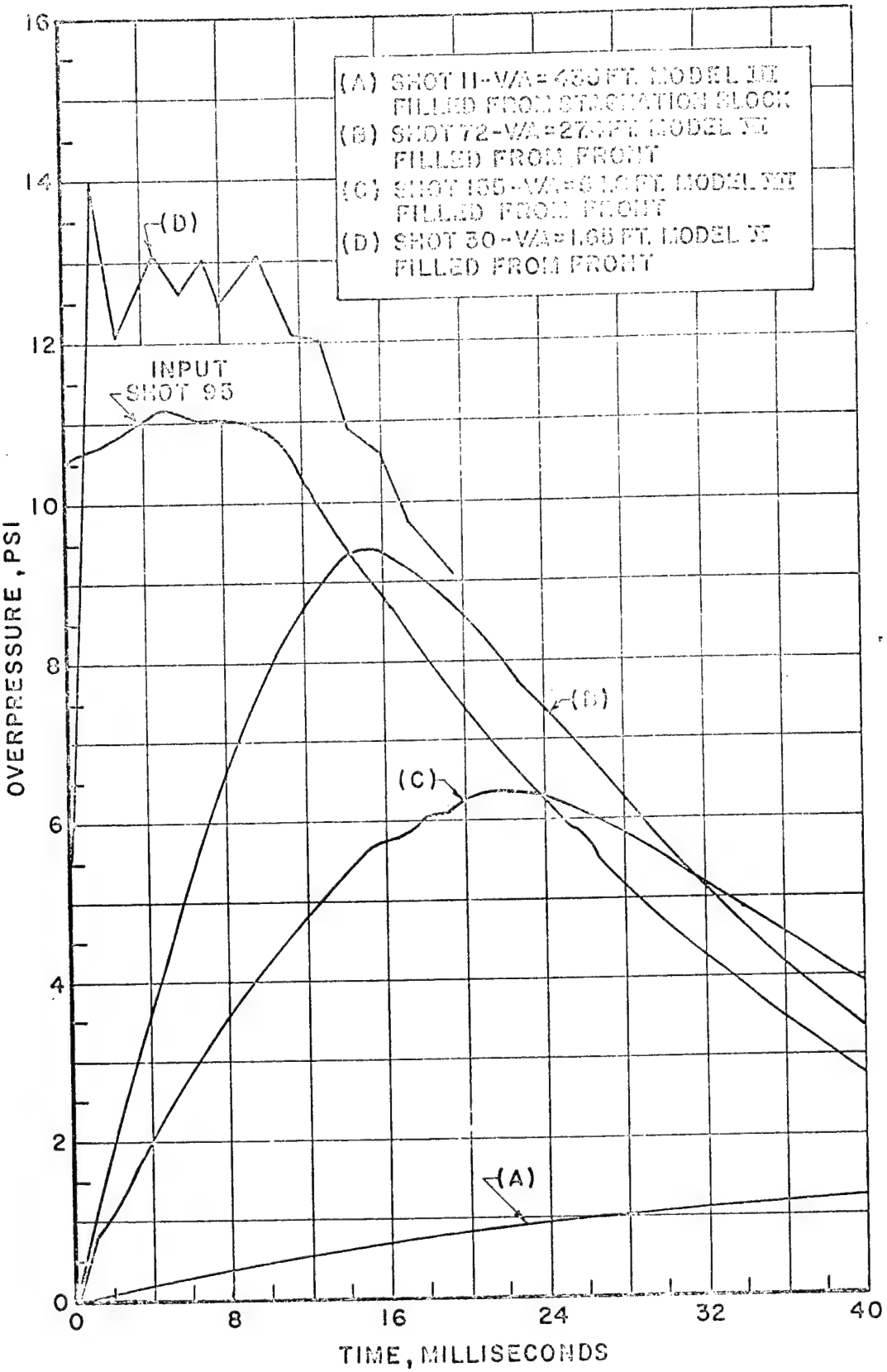

Figure 12. Comparison of filling as a function of model volume to entrance area ratio

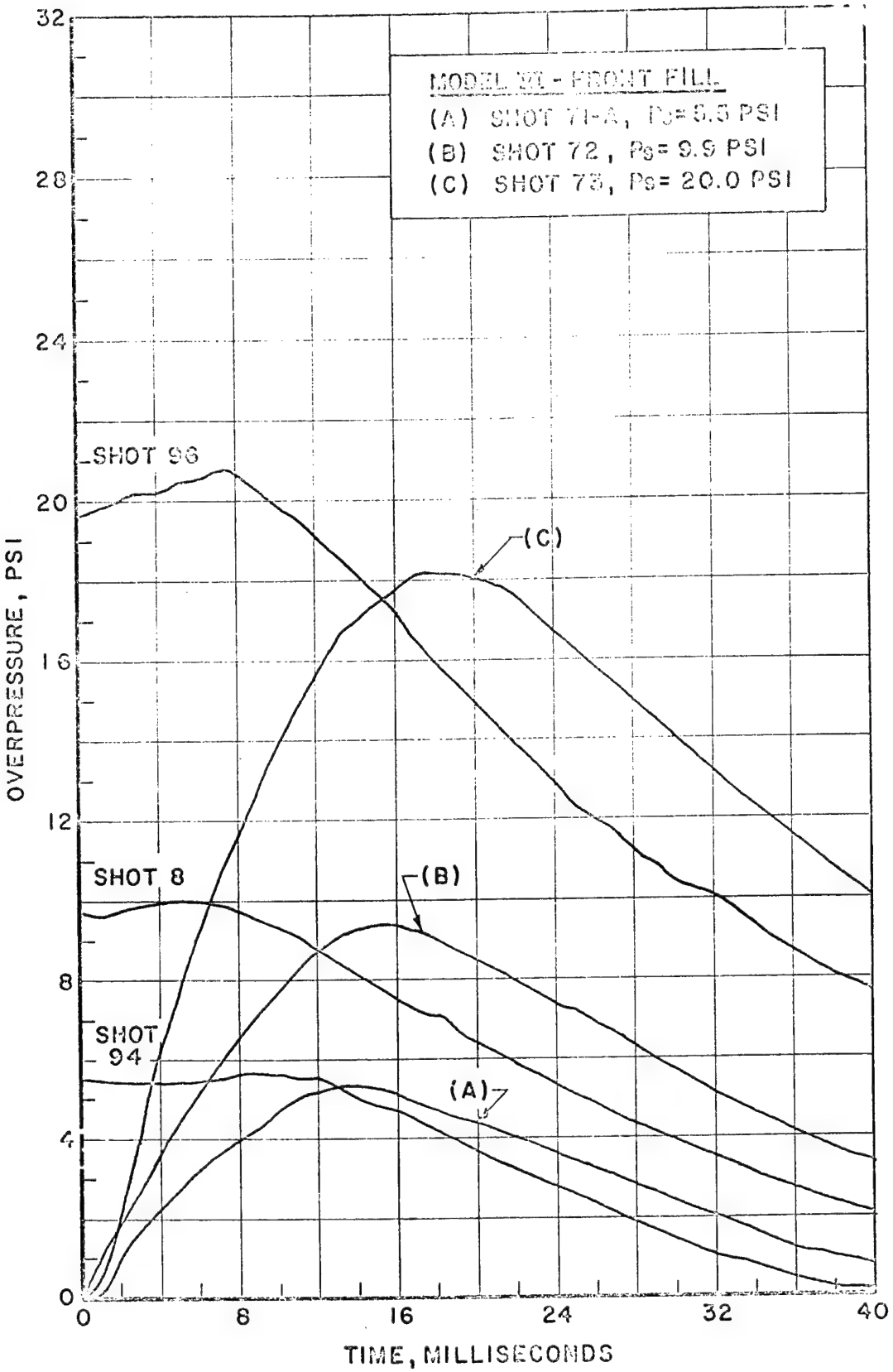

Figure 13. Comparison of filling as a function of input pressure

Figure 7 for typical stagnation records. The records plotted have all been smoothed for these comparisons and do not show the stepwise filling process that is present in the oscilloscope records, Appendix B. Reference 1 points out that stepwise filling is necessary to the mathematics model used in the computer predictions.

Figures 14-16 show filling results for input pressures 5.5-20 psi for Models VI, XI, XIII, and X. A single entrance, or two entrances of total area equal to the single entrance, behaved very much the same way in filling. The front and rear entrances caused a filling with a somewhat less maximum pressure at a greater fill time than did the front filling. There was also something of a greater fill rate during the first few milliseconds of filling for the lowest input pressure. The major difference in filling was apparent for the shielded model. Only about one-half the input pressure was reached for the 20 psi input; however, the fill time to the maximum remained about the same.

Figures 17-23 show comparisons between the two rooms and orientations for Model VII. The fill curves presented in Figures 17 and 18 for both rooms are quite similar, although shown in Figure 21 the second room fills to a little higher pressure (12 percent) than the first room at the 20 psi input pressure. Figures 19 and 20 show the comparison for the 20 psi input pressure. There is little difference for the 10 psi input pressure. Again as in the single room, Model VI, the front fill shown in Figure 21 gave the highest maximum pressure, rear-fill shown in Figure 22 was next, and side fill shown in Figure 23 was least. Figures 24 and 25 show results from Model VII for the two room entrances in-line, off-set (one at top and one at bottom, but on the same line), and a single room with the partition wall removed. The off-set entrances appear to cause the largest fill pressure and not much difference for in-line entrances compared with the single room.

Figures 26 and 27 show traces which compare the pressure loading as measured at the center of the external faces of Model VIII and the loading with a shield, Model X. The comparison shown is for an input pressure of 5.4 psi. Similar traces were observed for the 10 and 20 psi

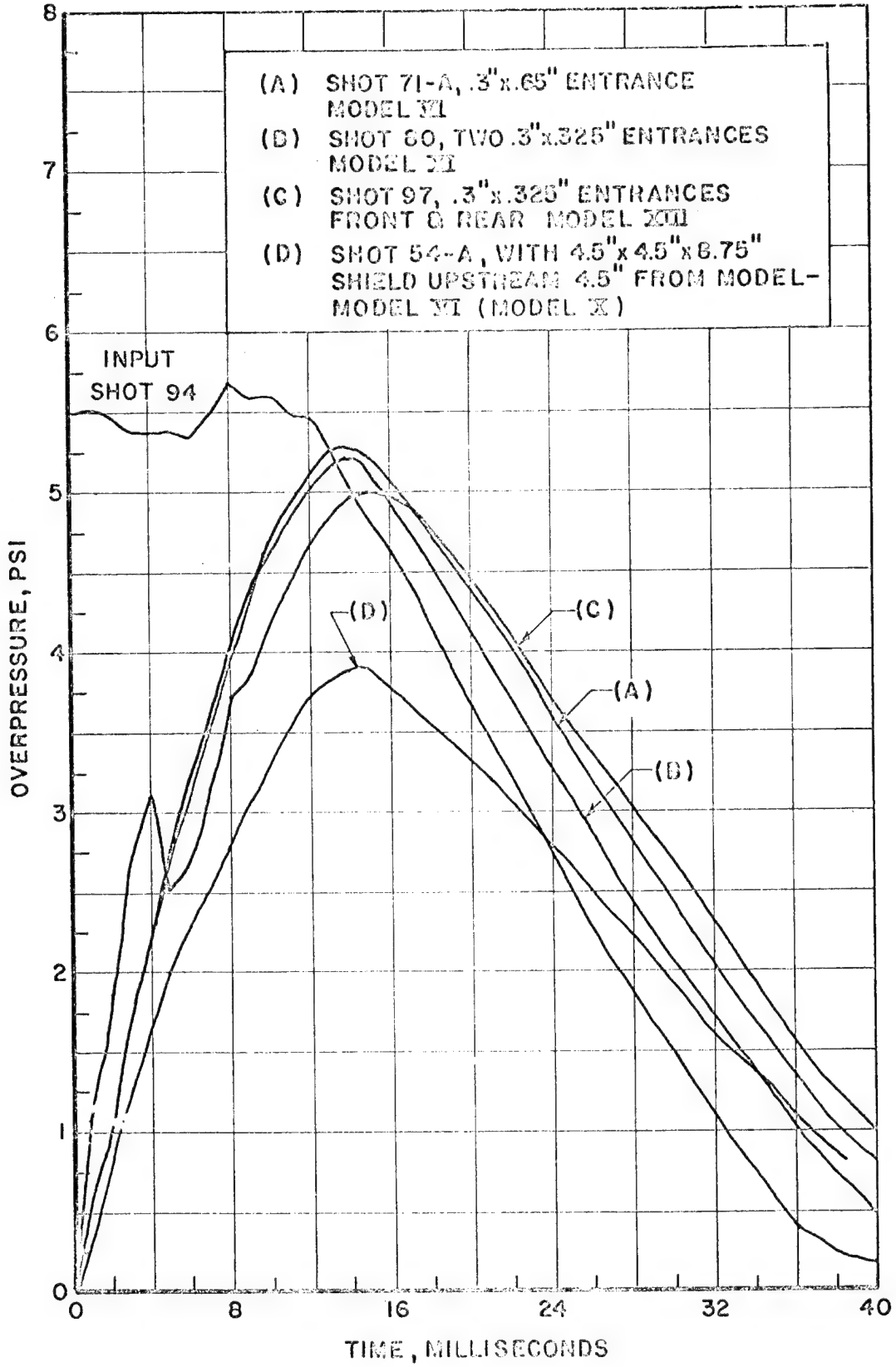

Figure 14. Comparison of filling as a function of entrance type, P_s = 5.5 psi

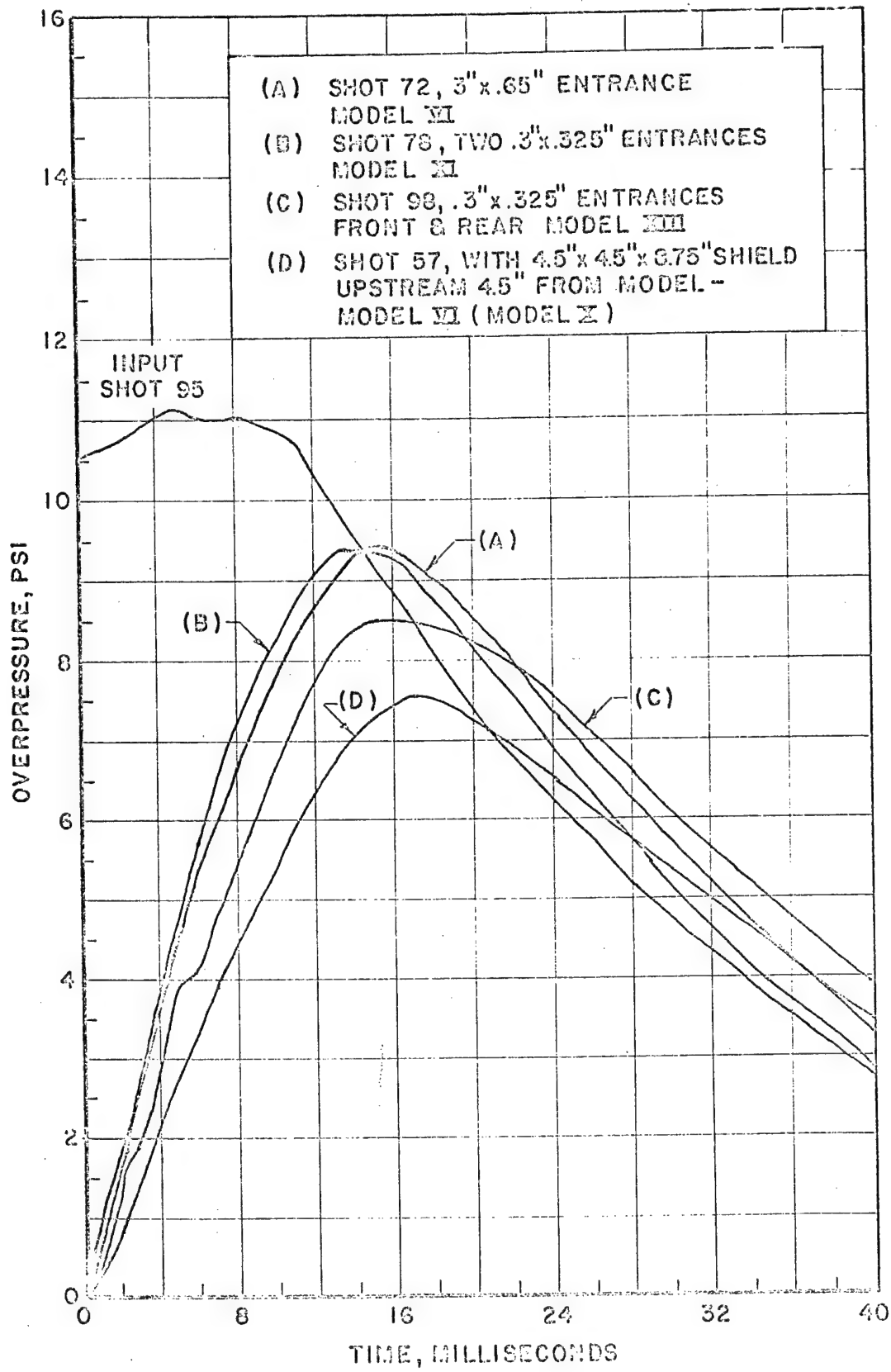

Figure 15. Comparison of filling as a function of entrance type, P_s = 10.8 psi

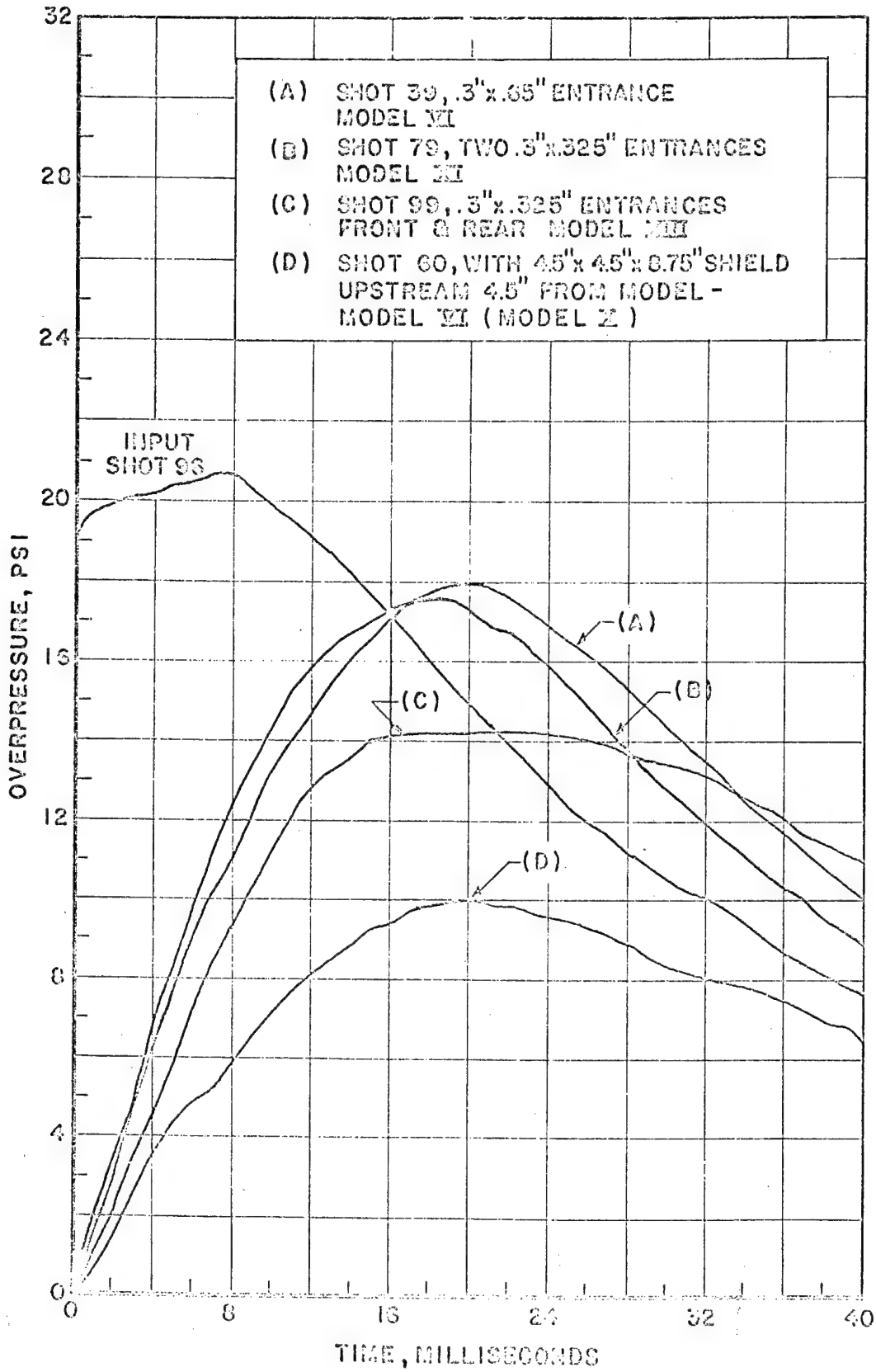

Figure 16. Comparison of filling as a function of entrance type, P_s = 20 psi

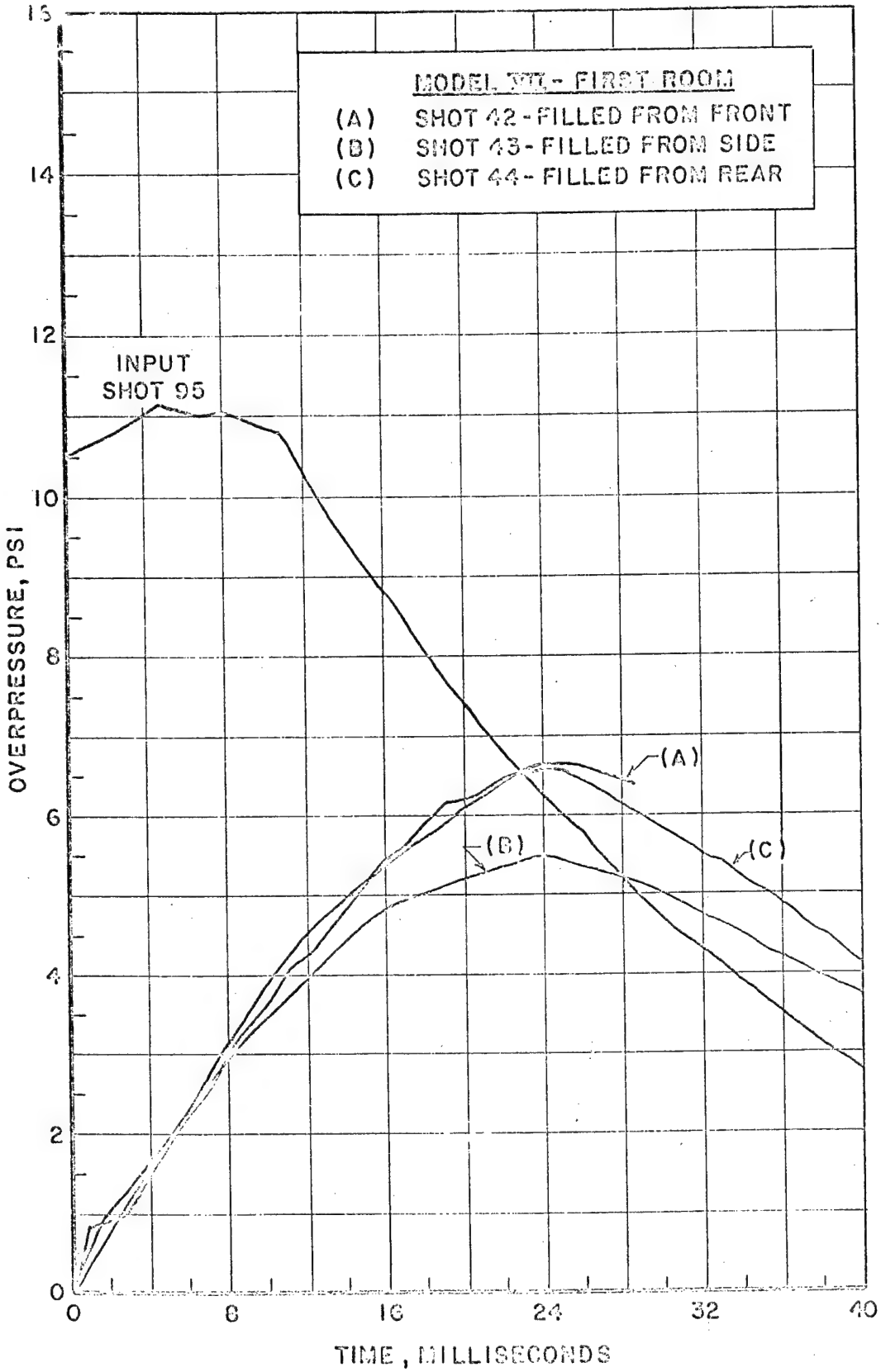

Figure 17. Comparison of entrance orientation for two-room model-gage in each room, P_s = 10.8 psi

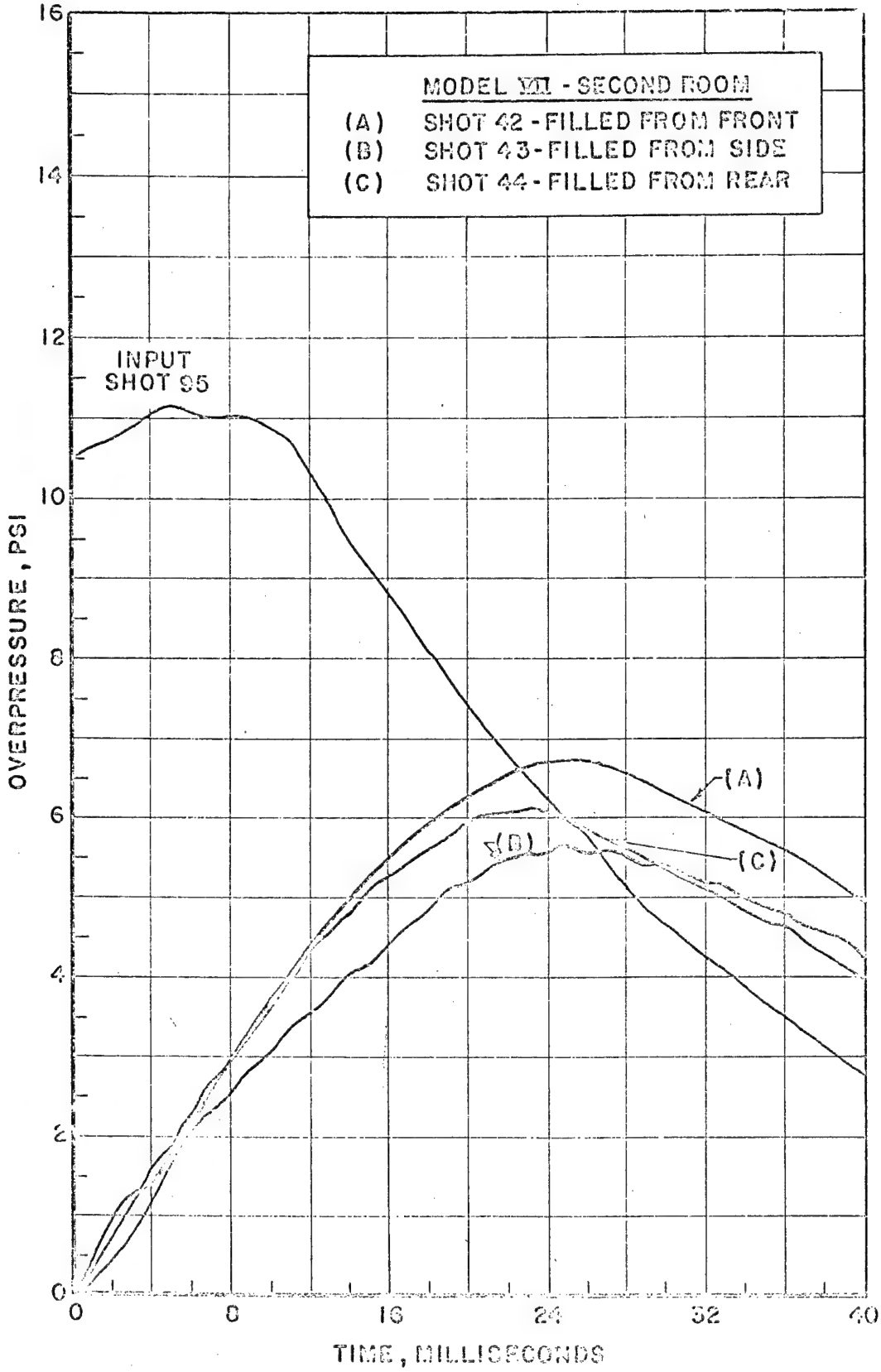

Figure 18. Comparison of entrance orientation for two-room model-gage in second room, P_s = 10.8 psi

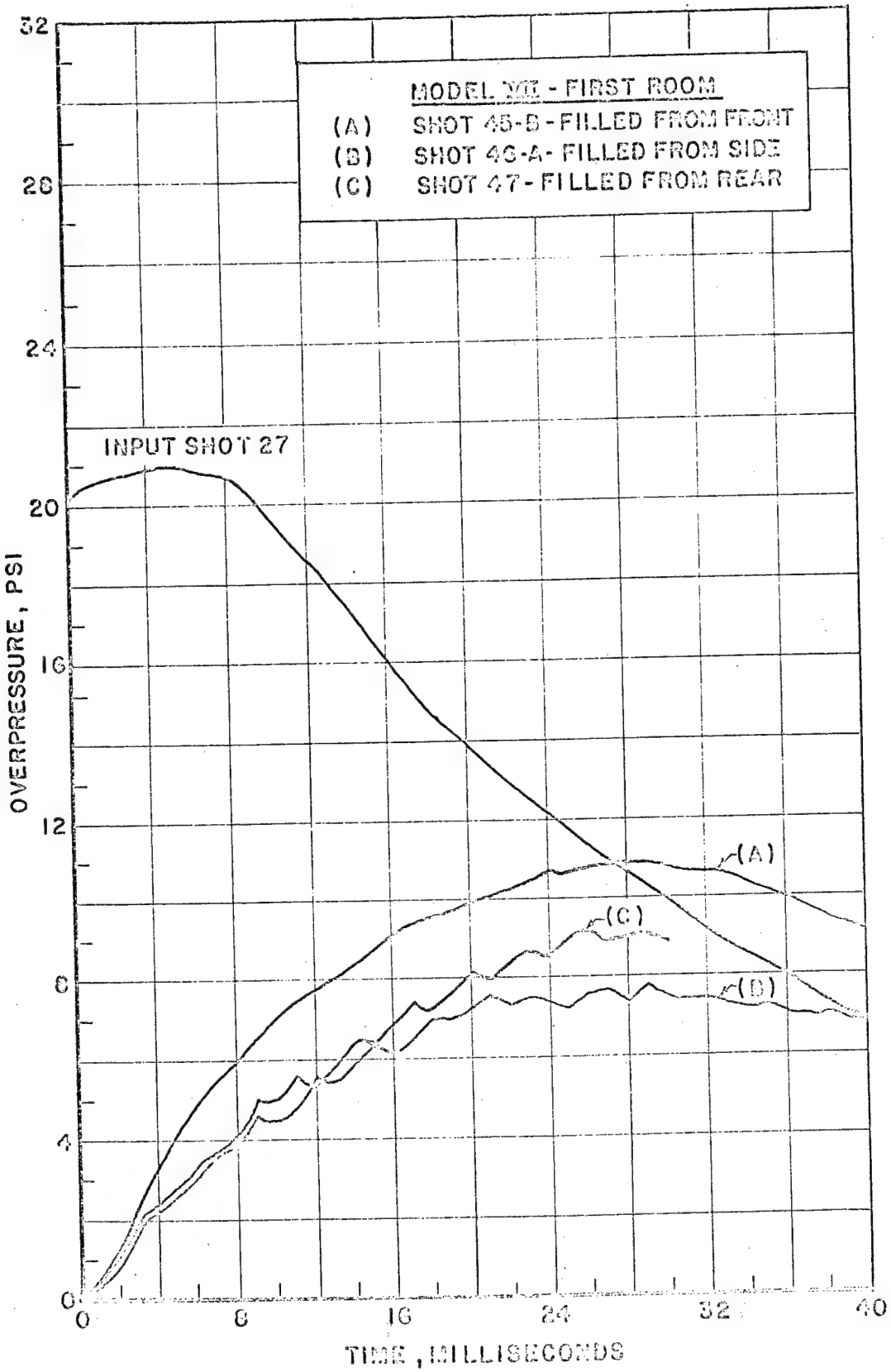

Figure 19. Comparison of entrance orientation for two-room model-gage in first room, P_s = 20.5 psi

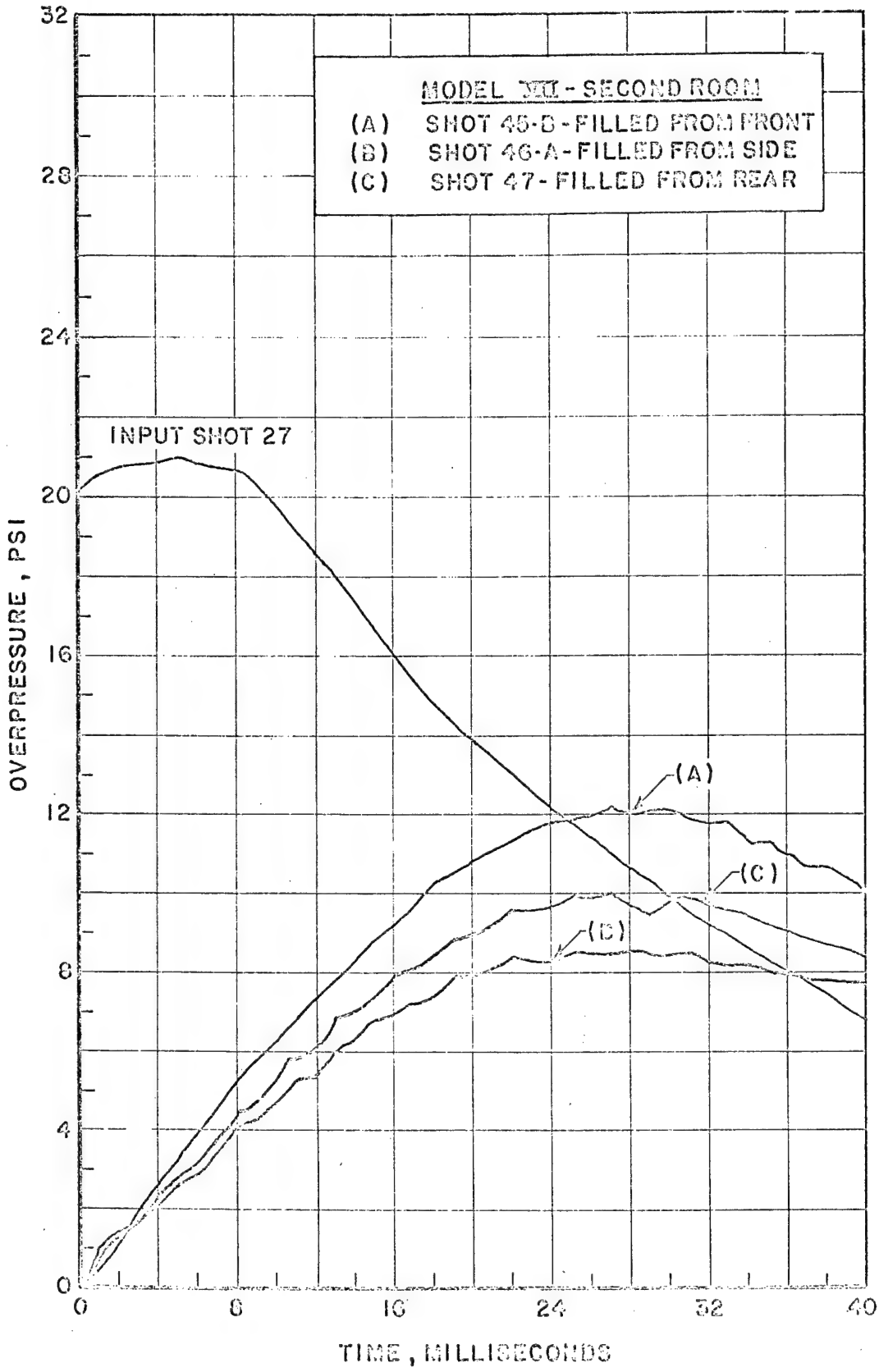

Figure 20. Comparison of entrance orientation for two room model-gage in second room, P_s = 20.5 psi

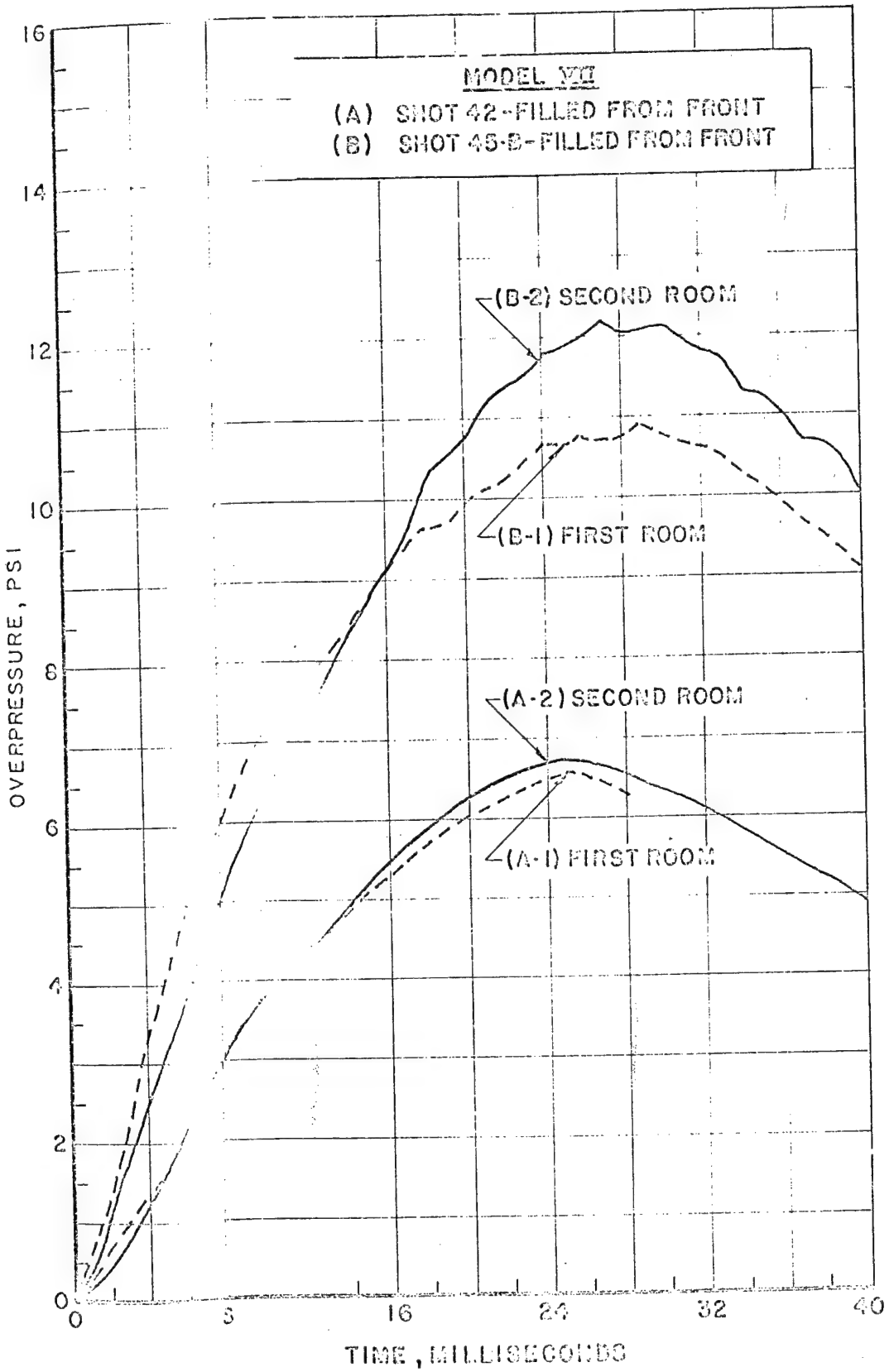

Figure 21. Comparison of front filling for each room of two-room model, P_s = 10.4 and 20.5 psi

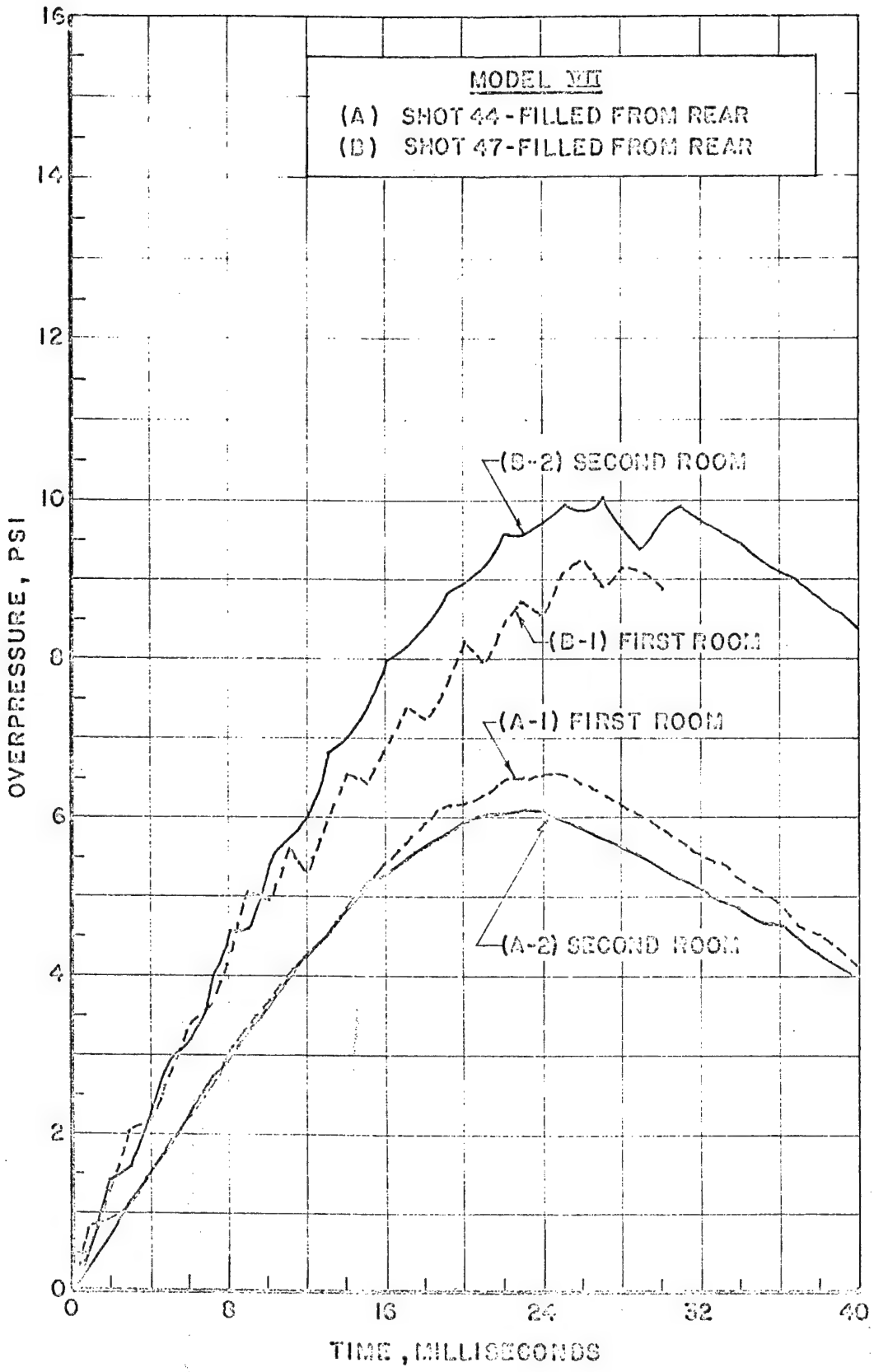

Figure 22. Comparison of rear filling for each room of two-room model, P_s = 10.9 and 20.6 psi

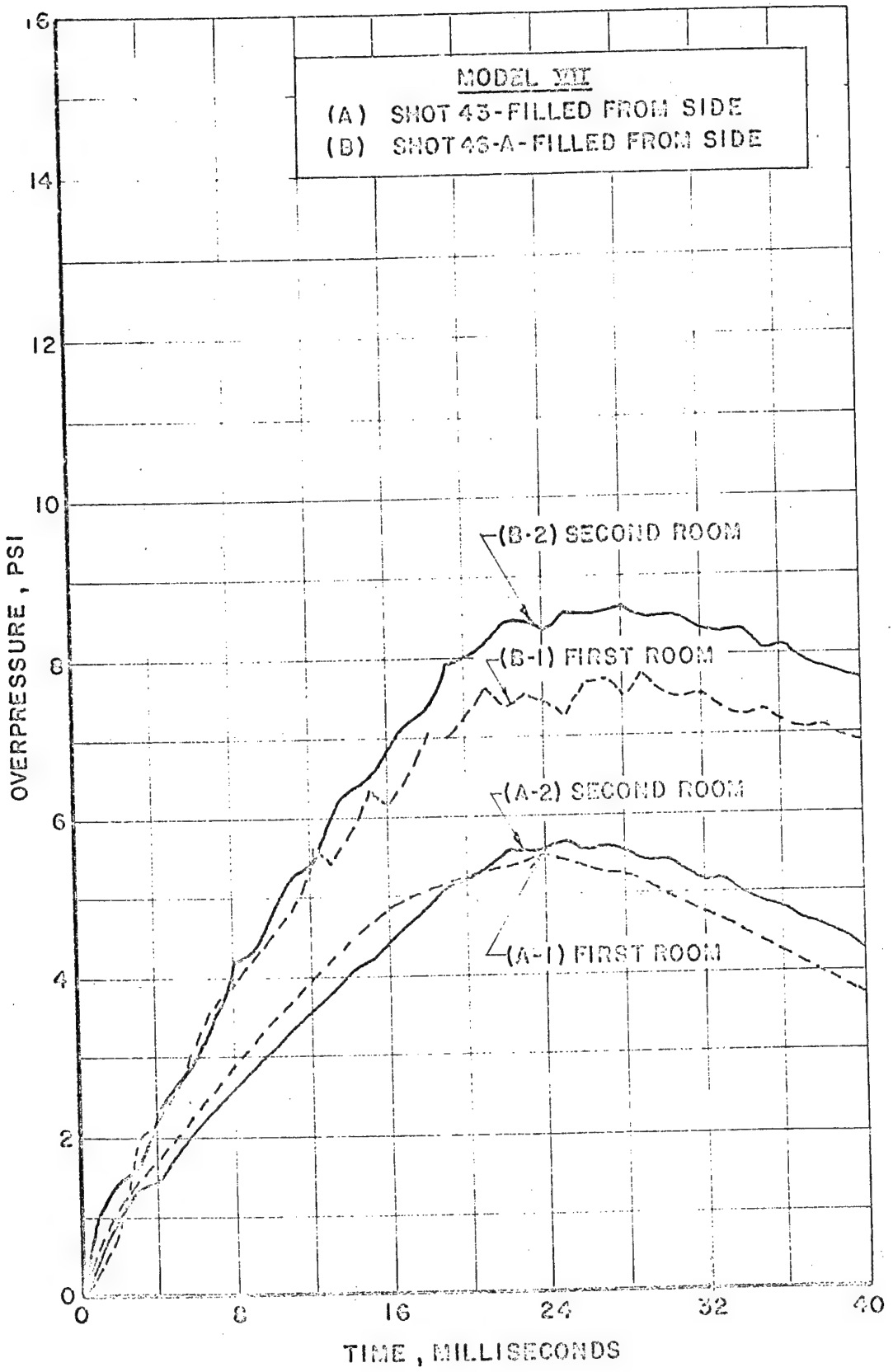

Figure 23. Comparison of side filling for each room of two-room model, P_s = 10.5 and 20.7 psi

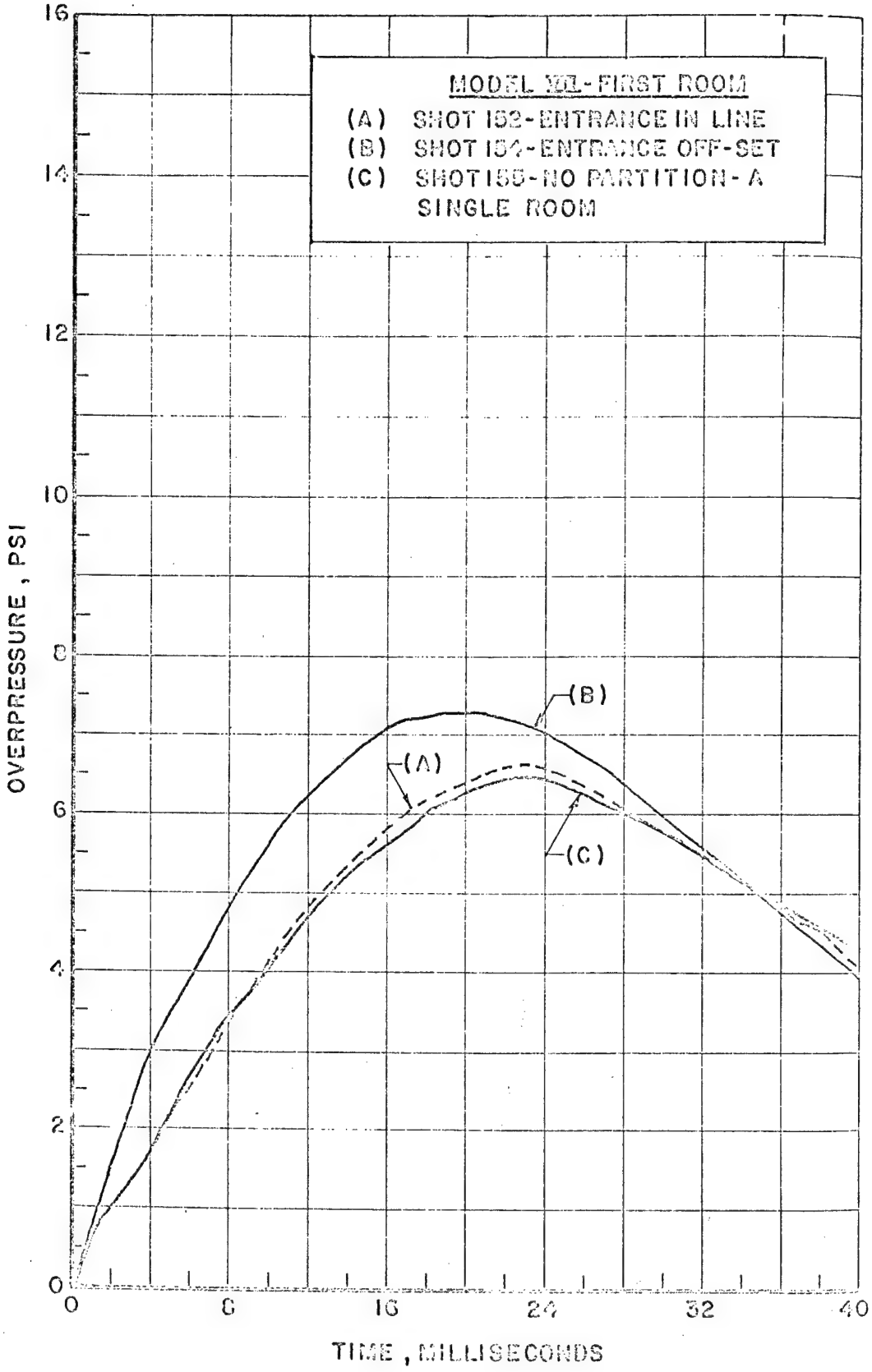

Figure 24. Comparison of filling of first room of two-room model P_s = 10.3 psi

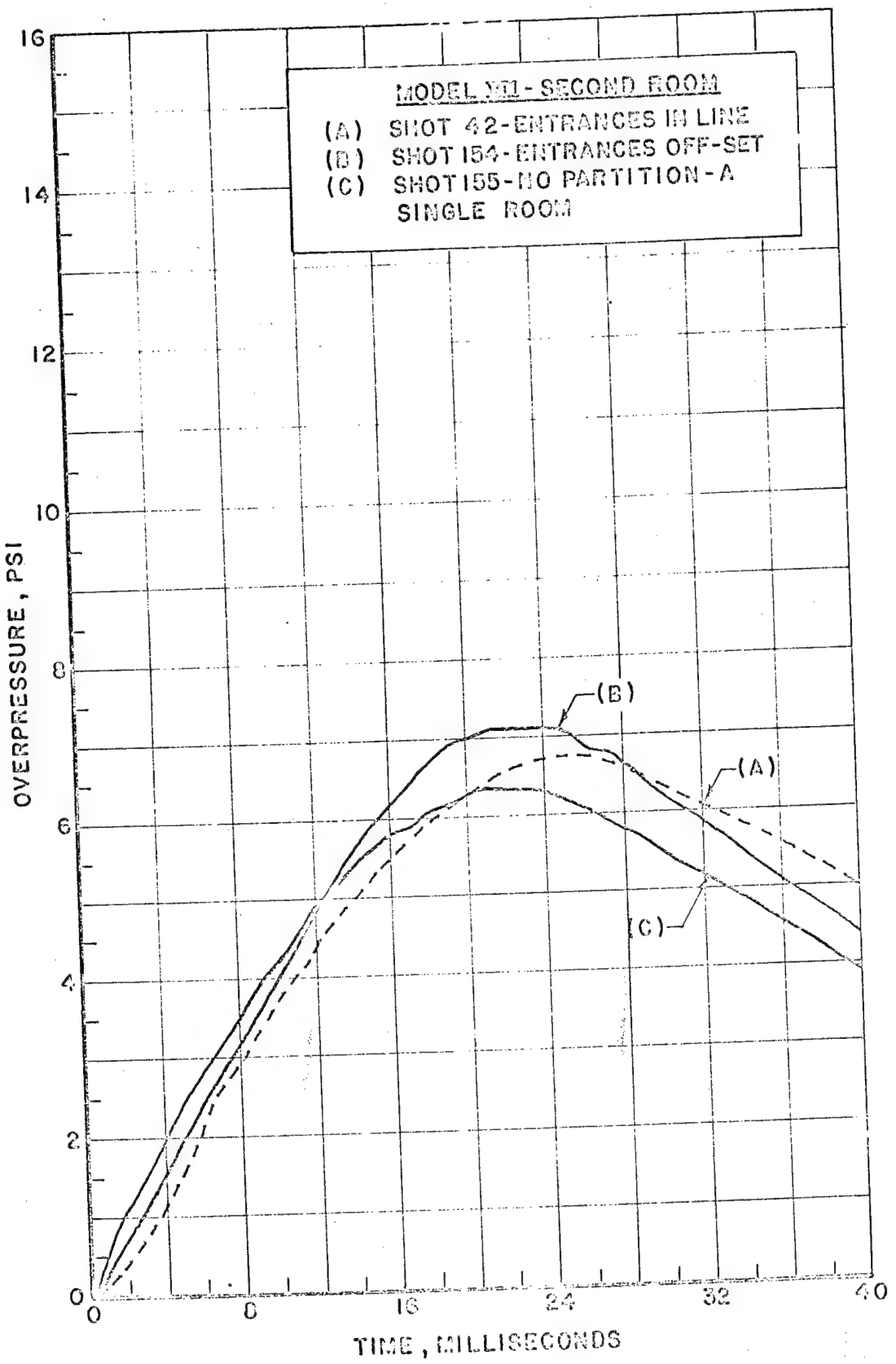

Figure 25. Comparison of filling of second room of two-room model P_s = 10.3 psi

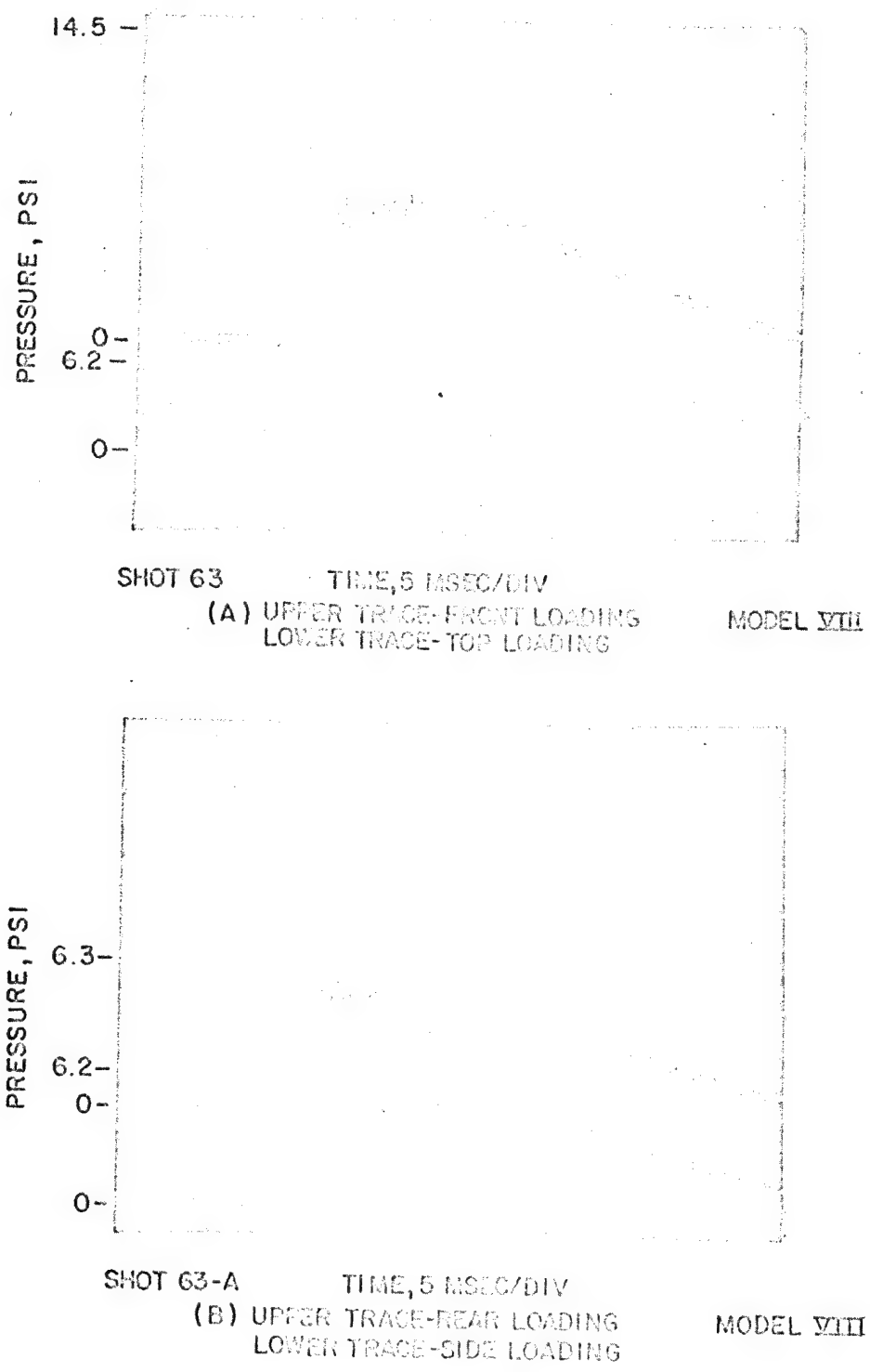

Figure 26. External pressure at center of faces of 4.5 in. cube - P_s = 5.4 psi

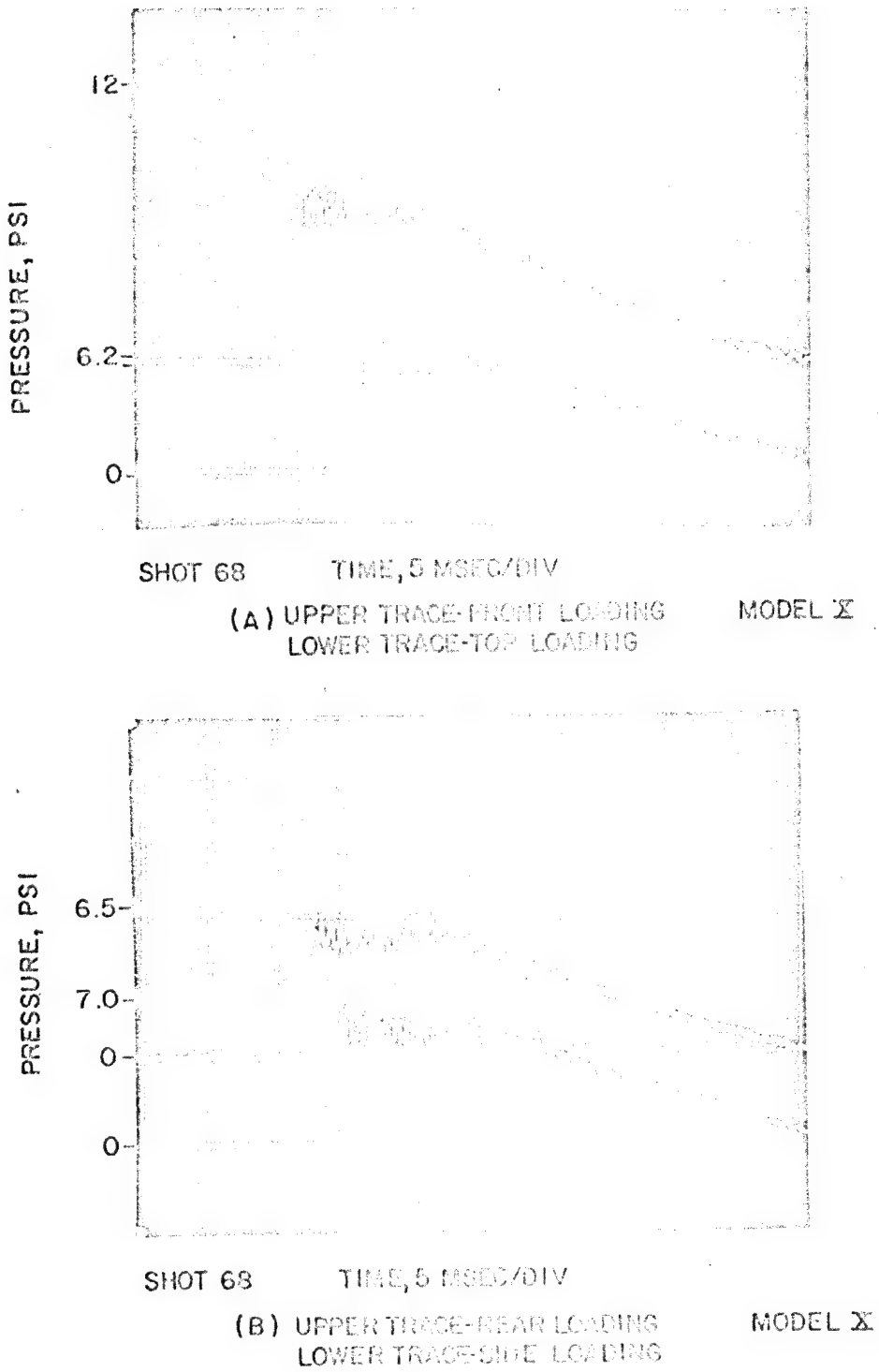

Figure 27. External pressure at center of faces of 4.5 in. cube with shield, P_s = 5.4 psi

inputs. See Appendix B. The unshielded model record shows an initial reflected pressure peak for the front face, oscillations, and an average semi-steady value near stagnation pressure. The rear, top, and sides all have similar pressure records with initial peaks above the side-on input pressure and a semi-steady value below the input.

The shield (Model X) caused the full reflected pressure peak on the front face to decrease but introduced additional oscillations in the pressure records from the other faces. Also, the semi-steady pressures were all somewhat above the values for the unshielded case.

The last in this three-dimensional model series to be discussed is Model XII. A group of ground position pressure readings were obtained upstream of a solid model, and models with entrances. The purpose of the transducer array (Refer back to Figure 6) was hopefully to define the area of stagnation pressure influence. The peak values of upstream reflected pressure and average pressure value (stagnation) are given. The reflected pressure varied depending upon whether an opening was present or not, but the average stagnation pressure seemed to be about the same over the entire array of transducer positions. See Appendix B for the pressure time records.

B. Two-Dimensional Models

Tables A-I and C-I, Appendices A and C, show the results from the filling of two-dimensional models with a step shock wave. Appendices A and C show the high speed photographs of the shock diffraction and flow process involved in the filling process, and the pressure time records from the models.

Figures A-13 of Appendix A will be used to point out the processes involved.

The shock wave approached Model XIV-D from the left, entered the 1 in. entrance, and expanded into the model with a cylinder shaped expansion. Vortices at the entrance were set up during this time. The shock front reflected from side walls, crossed the length of the model, reflected at the rear wall, and started the return crossing with Mach reflections at the side walls. By Frame 15, multiple shock interactions have occurred and turbulent jet flow appears to have occurred.

The nylon ball, upper left at entrance, has barely begun to move at this time. The motion in later frames may be followed by comparing the ball with the black grid lines marked in both directions on the photographs.

Figures 28 and 29 show distance-time plots of the center of the ball as it moved during the times shown in Figure A-13. Initially, the ball oscillates a little before getting started at about 300 μsec. After about 700 μsec, a steady average horizontal velocity of about 30 ft/sec is reached and a vertical rise of about 7 ft/sec after 200 μsec. (True vertical direction is toward bottom of photographs in order to retain proper frame-time sequence.)

The remainder of the shots of Model XIV with smoke grids were read and quantities of average velocity flow vectors, densities, and dynamic pressure were calculated by machine. The tabulated results and representative plots of velocities as a function of times are shown in Appendix D. It is seen from the tabulated results that velocities were measured from minimum values of a few feet per second to several hundred feet per second maximum, depending both on position within the model and time of measurement.

Table C-I gives the diffracted values of initially transmitted shock overpressure into the models. Note that a minimum of about 0.6 psi pressure and a maximum of about 1.6 psi were recorded for the 1/8 in. entrance of Model XIV-A. Values of pressure ranged from these to a minimum of about 1.3 psi, to a maximum of about 5.8 psi, for the double entrance of Model XIV-F. The double slit caused a Mach interaction between the two incoming diffracted shock fronts to create higher pressures than for the single 2 in. entrance.

C. Field Model

The pressure-time traces from the gages mounted in the field model (Model XV) are shown in Figures 30 and 31. The first figure, Figure 30, shows tracings of the input pressure as recorded by an electronic gage (Reference 4) (Trace A) in front of the model, (Refer back to Figure 9.)

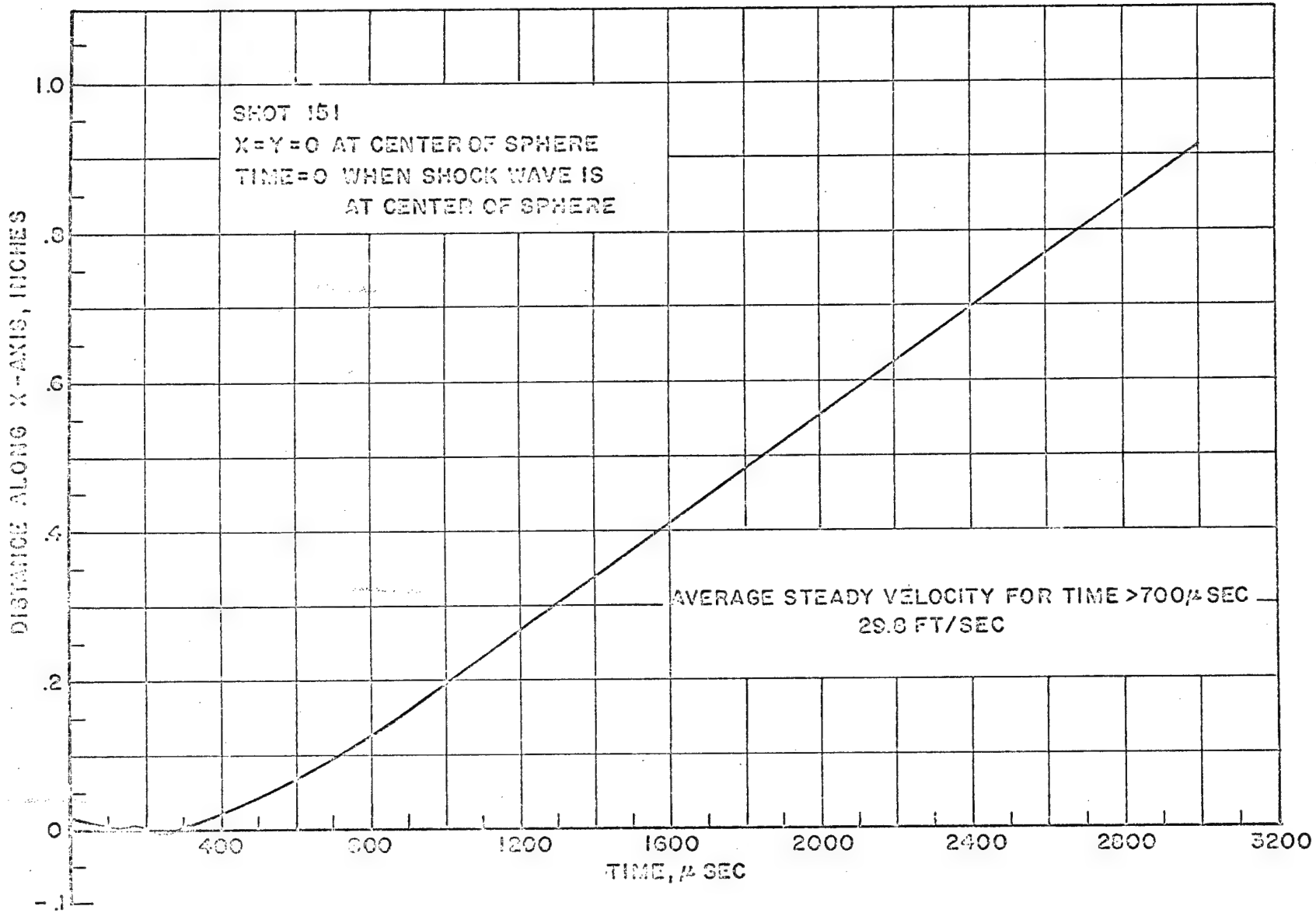

Figure 28. Horizontal motion of nylon sphere across Model XIV

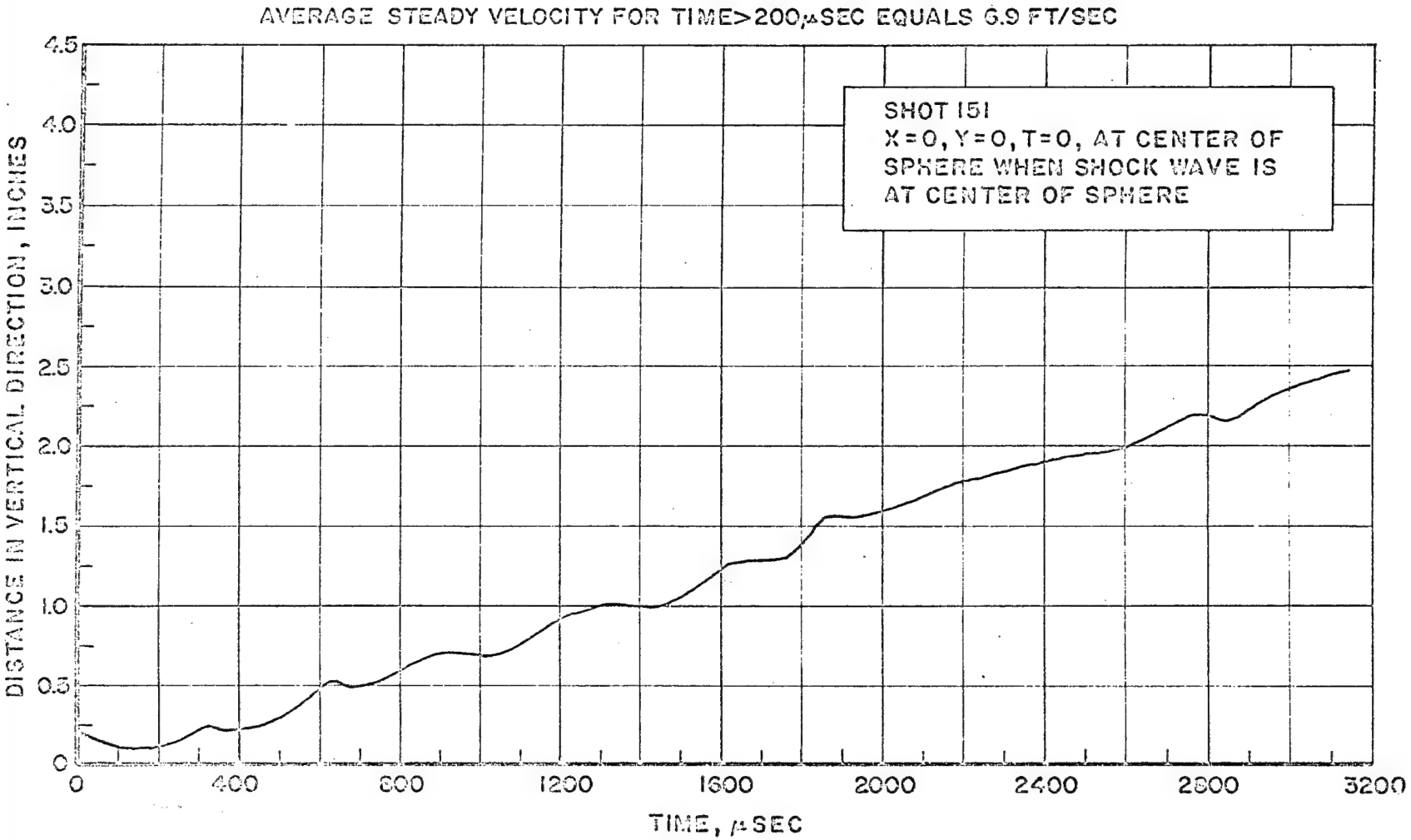

Figure 29. Vertical motion of nylon sphere as a function of time

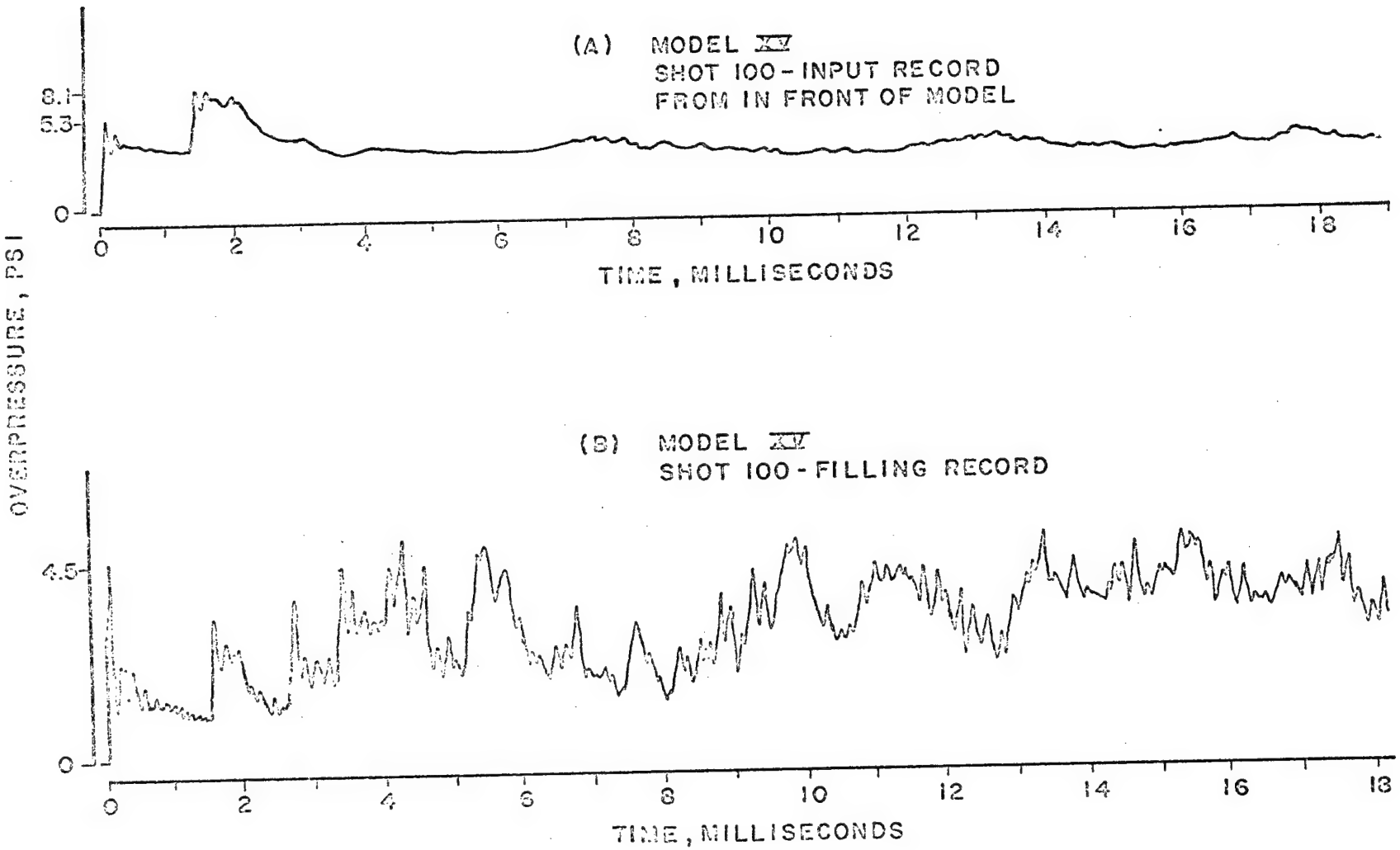

Figure 30. Filling of field Model XV

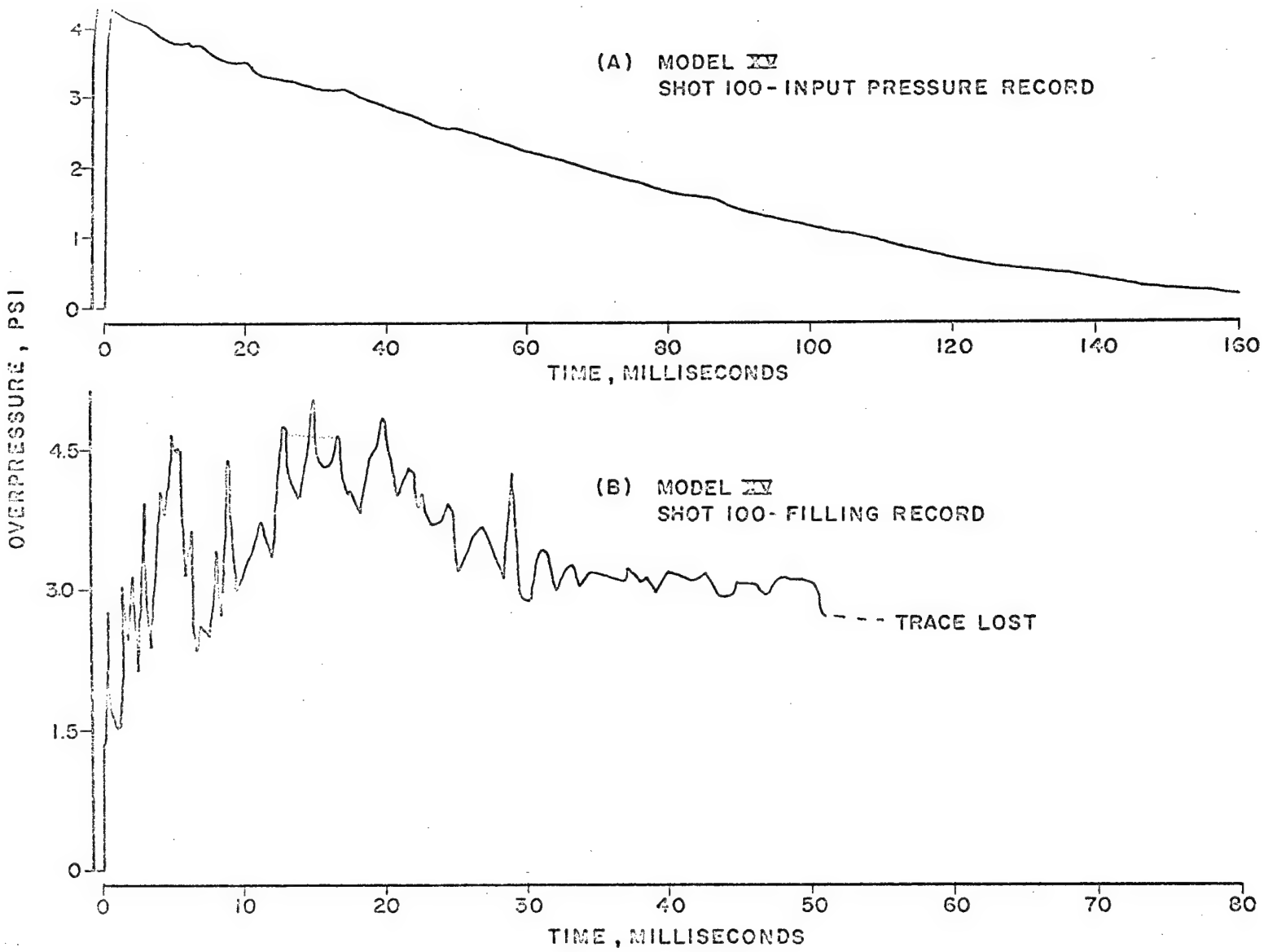

Figure 31. Machine smoothed pressure-time traces from Model XV

and the filling record from an electronic gage in the center of the interior bottom floor of the model (Trace B). Notice again, the peri step-wise type of filling which may be seen on the traces from the t dimensional models, given in Appendix C.

Figure 31 shows machine smoothed traces from self-recording pres capsule gages (Reference 4). Trace A is of the undisturbed input bla wave and Trace B is the filling record for the interior of the model. Trace B shows filling to about 4.5 psi at 15.5 msec which is nearly e to the initial input side-on overpressure.

The results of the field model seem to correspond to the filling mode as seen in the smaller model study in the shock tubes. See Figure 32 for a comparison of the filling of a 4 in. cube (Model VI) i the shock tube with the 3 ft cube (Model XV) used for the field shot. The smoothing of the filling curve from the shock tube model has obscu the incremental filling process which is seen in the filling of the fi model. This may be seen a little better in Figure 30 where the fillin trace has been expanded in time. Overfilling with respect to the input wave is present for both models. The field model shows a large initial pre-filling at about 5 msec which was not obvious with the smaller shoc tube model.

IV. SUMMARY AND CONCLUSIONS

Several two- and three-dimensional models of single and double rooms were tested under input shock waves of 5-20 psi peak overpressure in the BRL shock tubes. A larger model was exposed to the blast wave from the detonation of 100 tons of TNT. Model orientation to the shock waves; entrance sizes, shape, or number; input pressure; and number of rooms were varied to determine parameter importance in the shock wave filling process of the models.

From a study of photographs and pressure-time traces the following conclusions are valid for the 5-20 psi overpressure range tested.

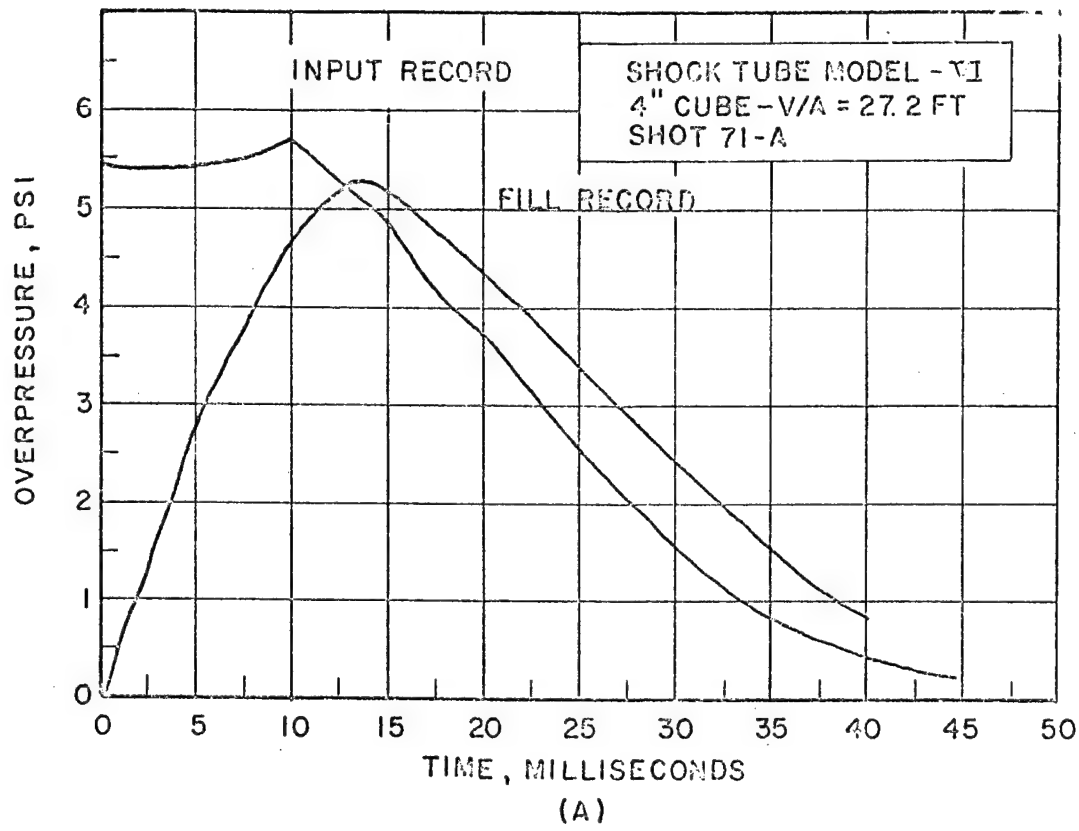

(A)

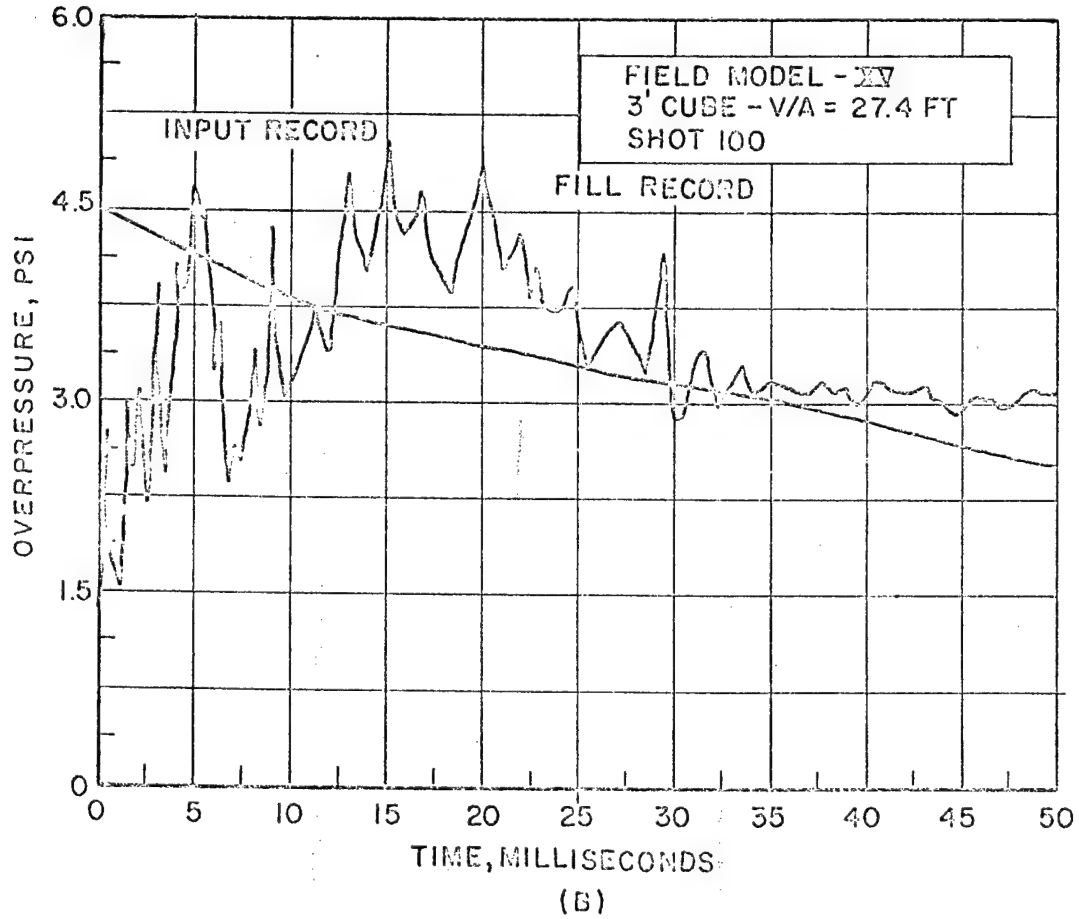

(B)

Figure 32. Comparison of filling for shock tube and field models

A. Three-Dimensional Models

1. For a constant volume to entrance area ratio (V/A), filling through an entrance in a stagnation block corresponds approximately to filling the model through a front entrance for a model exposed head-on to the shock wave.

2. Side-on filling, such as the shock wave does when passing side on past a short tunnel entrance leading to a model outside the shock tube, corresponds approximately to filling from a rear entrance, for a model of same V/A filled inside the shock tube.

3. Filling from the side entrance for an exposed model gives the lowest maximum fill pressure and lowest rate of fill compared to front or rear filling for a given input wave.

4. For increasing values of V/A, the time to maximum filling increases. Note, however, that if the input wave has a long duration compared to the model fill time, the model will eventually overfill to a value greater than the outside pressure existing at that particular time.

5. The fill time to maximum pressure became longer as the input shock overpressure was increased, from 13.7 msec for P_s = 5.3 psi to 17.2 msec for P_s = 19.6 psi. Also, the model filled to a pressure greater than the pressure outside during the decaying phase of the input shock wave; for example, overfilling occurs from a time of about 12 msec to the end of the recording time for the 10 psi input wave.

6. The filling from two front entrances is similar to that from one entrance for the same V/A for the model and a single entrance in both front and rear caused a longer fill time to maximum pressure.

7. The fill curves for each room of a two-room model were very similar, although the second room filled to about 12 percent higher than the first room for P_s = 20 psi. In-line entrances acted about the same as if the partition between the rooms were removed.

8. The shielded model filled to a lower pressure than the unshielded model.

9. The external center face loading, for the single cube el without entrances, showed on the front surface a reflected pressure, illations, and an average semi-steady pressure equal to about the agnation value measured by the pitot tube transducer for a given input e. The rear, top, and side faces showed initial pressures above the e-on input value and an average semi-steady value below the input ssure.

10. The effects of the shield upon the exterior loading were lower the reflected pressure spike on the front surface, cause itional pressure oscillations, and to raise the value of the semi-ady pressure on all the faces of the model.

11. A uniform stagnation pressure field corresponding to the ut pressure was found to exist to 3 in. in front of a 4.5 in. high ic model. (Model XII, Table B-I).

Two-Dimensional Models

1. The shock filling process consisted of the shock wave ffraction into the model through the entrance, vortices which were set at entrance, multiple reflections which occurred from all the interior ls, and a jet which seemed to be established from the entrance into model.

2. Particle velocity vectors were calculated with magnitudes to several hundred feet per second within the model. Others of ying magnitudes and directions were computed.

3. One-eighth inch diameter nylon balls obtained horizontal ds of about 30 ft/sec and vertical speeds of about 7 ft/sec for input pressures of approximately 5 psi.

4. Transmitted shock front pressures increased with entrance h. Values were measured from less than 1 psi to 5.8 psi on the all of Model XIV.

C. Field Model

1. Multiple reflections were seen corresponding to the results from the shock tube models.

2. A periodic type of filling was observed as in the smaller models.

3. The initial transmitted (diffracted) shock wave, measured at the center of the model, retained the outside peak pressure because of the large area of the entrance. For entrance sizes of 1 in. and greater, shock tube Model XIV also transmitted diffracted pressures equal to the input overpressure.

4. The model filled similarly to the smaller model of the same V/A, with respect to pressure and fill time, after a crossing time correction was made.

ACKNOWLEDGMENTS

The author wishes to thank Mr. Harry Pearce for his assistance with the experiments, Mrs. Helen Malone and Mrs. Buckner Pannill for processing the data for the computer, and Mr. William Matthews for assisting in the preparation of the many figures needed for the report.

REFERENCES

1. Joseph Melichar, "The Propagation of Blast Waves into Chambers: Aerodynamic Mechanisms," Final Progress Report for Office of Civil Defense, Work Order No. DARC 20-67-W-0153, November 1967, Ballistic Research Laboratories Memorandum Report to be published.

2. George A. Coulter, and Robert L. Peterson, "Design of Aircraft Revetments," Ballistic Research Laboratories Memorandum Report No. 1440, October 1962.

3. George A. Coulter, "Dynamic Calibration of Pressure Transducers at the BRL Shock Tube Facility," Ballistic Research Laboratories Memorandum Report No. 1843, May 1967.

4. Louis Giglio-Tos, *et al*, "Air Blast Parameters from Summer and Winter 20-Ton TNT Explosions Operation Distant Plain (Defence Research Establishment, Suffield, Ralston, Alberta, Canada)," Ballistic Research Laboratories Memorandum Report No. 1894, November 1967.